GJO–2002– 322–TAR

# Hanford 200 Areas Spectral Gamma Baseline Characterization Project

# 216-B-35 to -42 Trenches Waste Site Summary Report

May 2002

U.S. Department of Energy

*Work Performed Under DOE Contract Number DE–AC13–96GJ87335 for the U.S. Department of Energy*

GJO-2002-322-TAR

**Hanford 200 Areas Spectral Gamma Baseline Characterization Project**

# 216-B-35 to -42 Trenches Waste Site Summary Report

**June 2002**

Prepared for
U.S. Department of Energy
Idaho Operations Office
Grand Junction Office
Grand Junction, Colorado

Prepared by
MACTEC-ERS
Grand Junction Office
Grand Junction, Colorado

Approved for public release; distribution is unlimited.
Work performed under DOE Contract No. DE-AC13-96GJ87335.

# Contents

# Contents (continued)



## List of Figures

# Contents (continued)



## List of Tables

**Hanford 200 Areas Spectral Gamma Baseline Characterization Project**
**216-B-35 to -42 Trenches Waste Site Summary Report**

**Prepared by:**

S.M. Sobczyk
MACTEC-ERS, Hanford

June 6, 2002
Date

**Concurrence:**

R.G. McCain, Hanford Technical Lead
MACTEC-ERS, Hanford

6-6-02
Date

C.J. Koizumi, Technical Lead
MACTEC-ERS, Grand Junction Office

6-10-02
Date

**Approved by:**

J.F. Bertsch, Project Manager
MACTEC-ERS, Hanford

6/10/02
Date

M.C. Butherus, Task Order Manager
MACTEC-ERS, Grand Junction Office

6-10-02
Date

J. Berwick, Project Manager
U.S. Department of Energy
Grand Junction Office

6-17-02
Date

J.M. Silko, Project Manager
U.S. Department of Energy
Richland Operations Office

06.18.02
Date

# Executive Summary

The U.S. Department of Energy Richland Office (DOE-RL) tasked the DOE Grand Junction Office (DOE-GJO) to conduct a baseline characterization of the gamma-ray-emitting radionuclides distributed in vadose zone sediments in the vicinity of waste sites in the Central Plateau (200 East and West Areas) of the Hanford Site.

The Spectral Gamma Logging System (SGLS) was used to collect data in existing boreholes and monitoring wells and to log new boreholes and wells being drilled as part of ongoing site investigation projects. This system uses a high-purity germanium (HPGe) detector to acquire high-resolution, gamma-energy spectra that allow detection, identification, and quantification of gamma-emitting radionuclides.

This report documents SGLS results obtained from eleven boreholes and three groundwater wells that surround the 216-B-35 to -42 Trenches, including six new boreholes drilled along the 216-B-38 Trench as part of the 200-TW-1 Remedial Investigation. Cesium-137 ($^{137}$Cs) was detected in every borehole in the vicinity of these trenches. Three intervals of $^{137}$Cs contamination were identified: (1) 0.3 to 10 pCi/g within 12 feet (ft) of the top of casing (TOC) reference mark; (2) 0.3 to $10^5$ picocuries per gram (pCi/g) at log depths between 10 and 70 ft; and (3) 0.3 to 3.5 pCi/g in a zone immediately above the current intercepted groundwater table. High gamma-ray intensities that saturated the SGLS detector were measured in nine vadose zone boreholes and one groundwater monitoring well between depths of about 10 and 70 ft. These intervals were logged with the High Rate Logging System (HRLS). The maximum detected $^{137}$Cs activity was approximately $2x10^5$ pCi/g beneath the 216-B-38 Trench in borehole C3342 at a depth of 16.5 ft. The deepest $^{137}$Cs concentrations were detected at the bottom of groundwater monitoring well 299-E33-21, where a maximum activity of 45 pCi/g was measured at 280 ft. Cobalt-60 ($^{60}$Co) was detected at the 216-B-36 and -38 Trenches and north of the 216-B-41 Trench in the interval from 30 to 72 ft at activities ranging up to 0.6 pCi/g. $^{60}$Co was detected below the groundwater table intercept in all of the groundwater wells at activities ranging from 0.1 to 0.3 pCi/g. Antimony-125 ($^{125}$Sb) was detected in groundwater monitoring well 299-E33-8 at log depths between 32 and 34 ft at activities ranging from 1 to 2.5 pCi/g. Europium-154 ($^{154}$Eu), europium-152 ($^{152}$Eu), uranium-238 ($^{238}$U), and uranium-235 ($^{235}$U) were not detected in any of the boreholes.

A comparison between the recently collected log data and spectral gamma data collected in the 1990s (seven boreholes) shows good agreement in apparent $^{60}$Co and $^{137}$Cs concentrations. Where comparisons could be made, significant changes in contaminant profile are not evident during the last 10 years. A review of historical gross gamma logs suggests that groundwater in the area may have contained fission waste products as early as 1957. Review of historical gross gamma logs, recent logging results for groundwater monitoring well 299-E33-21, and the total discharge volume indicate the discharges to the 216-B-37 Trench most likely reached groundwater. The Hanford H1/H2 contact, a potential spreading surface, was mapped to predict the direction of lateral migration in the vadose zone. Recommendations include the installation of additional boreholes east of the 216-B-38 Trench and north of the 216-B-41 Trench to define the extent of lateral spreading of contaminants discharged to the soil column, and the installation of a borehole to groundwater near the eastern end of the 216-B-37 Trench.

# 1.0 Introduction

The Hanford 200 Areas Spectral Gamma Baseline Characterization Project operates borehole geophysical logging equipment to measure naturally occurring and anthropogenic radionuclides in the subsurface in the vicinity of 200 Area waste sites. The following sections provide brief discussions of background, project purpose and scope, field and technical methods, and project objectives.

## 1.1 Background

The U.S. Department of Energy (DOE) Hanford Site encompasses approximately 1,450 $km^2$ (560 $mi^2$) in the Columbia Basin of south central Washington State. Beginning in World War II, the Hanford Site was involved in production of plutonium to support the national nuclear weapons program. The Hanford Site is subdivided into a number of operational regions identified as the 100, 200, 300, and 1100 Areas (Figure 1). In 1989, the U.S. Environmental Protection Agency (EPA) placed these areas on the National Priorities List (NPL) pursuant to the *Comprehensive Environmental Response, Compensation, and Liability Act of 1980* (CERCLA). The 200 Areas, located on a plateau near the center of the Hanford Site, consist of the 200 West Area and 200 East Area, which include waste management facilities and inactive irradiated-fuel reprocessing facilities, and the 200 North Area, which was formerly used for interim storage and staging of irradiated fuel.

## 1.2 Purpose and Scope of Project

The goal of the DOE Grand Junction Office (DOE-GJO) Hanford 200 Areas Spectral Gamma Baseline Characterization Project is to collect data from existing boreholes and determine the present nature and extent of contamination associated with gamma-ray-emitting radionuclides distributed in the subsurface in the vicinity of 200 Area waste sites. The waste sites include soil waste sites (and associated structures such as pipelines) resulting from the discharge of radioactive liquids and solids from processing facilities to the ground (via ponds, ditches, cribs, and burial grounds); the peripheral regions of the single-shell waste storage tank farms where leakage of high-level radioactive waste constituents from specific tanks may have migrated; and regions where unplanned releases of radioactive liquid wastes have occurred. Most of the soil waste sites and all of the unplanned release sites have been assigned to the Environmental Restoration (ER) Program. A small percentage of the soil waste sites and the peripheral regions of the tank farm sites have been assigned to the DOE Office of River Protection (DOE-ORP).

The purpose of the Hanford 200 Areas Spectral Gamma Baseline Characterization Project is to present spectral gamma data collected from existing boreholes in and adjacent to waste sites in the Hanford 200 Areas. High-resolution gamma-energy spectra are collected in these boreholes using consistent and defensible methodology. This work effectively extends the existing baseline data set developed for the Hanford single-shell tank farms into the surrounding areas occupied by liquid and solid waste sites. The baseline data are evaluated to determine the source(s) of the contamination, to develop a dataset that can be used to evaluate future changes, and to correlate the geophysical signature of known and presumed geologic features that may affect radionuclide migration. This information is needed to manage the sites and to make informed decisions about site remediation. "Depth of penetration and extent of lateral spread of radionuclides beneath a waste disposal facility

depend upon the volume and type of waste discharged and the stratigraphic, physical and chemical characteristics of the earth material beneath the site" (Raymond and McGhan 1964).

Gamma spectra from each borehole are analyzed to determine concentrations of naturally occurring radionuclides potassium-40 ($^{40}$K), thorium-232 ($^{232}$Th), uranium-238 ($^{238}$U), and associated decay progeny, as well as man-made gamma-emitting radionuclides such as cesium-137 ($^{137}$Cs), cobalt-60 ($^{60}$Co), and europium-152/154 ($^{152/154}$Eu). Variations in naturally occurring radionuclides are also useful in stratigraphic correlation.

The Spectral Gamma Logging System (SGLS) is used to acquire spectral gamma-ray data from boreholes and wells related to the 200 Area waste sites. Intervals of high gamma-ray intensity are logged with the High Rate Logging System (HRLS).

This project is limited in scope to passive spectral gamma-ray logging. As a result, only radionuclides that decay with the emission of gamma-ray photons can be detected and quantified. Furthermore, only existing boreholes/wells and any new boreholes drilled for other projects are logged. No new borehole drilling is specified or planned as a part of this project, although recommendations for additional boreholes may be provided when appropriate. Additional details regarding the scope and general approach to this characterization program are included in the baseline characterization plan (DOE 2001c) and project management plan (DOE 2001b).

Specific activities under this project include preparation and maintenance of a database of existing boreholes and geophysical log data, logging existing boreholes with the SGLS and HRLS, analysis and plotting of log data, and preparation of reports. Because many waste sites are the subjects of site characterization efforts in RI/FS work plans, well logging is performed in existing and new boreholes to support these activities and data are provided for incorporation into the Remedial Investigation Reports.

## 1.3 Methods

The following sections discuss field and technical methods used by the Hanford 200 Areas Spectral Gamma Baseline Characterization Project that have been specifically developed for high-resolution borehole measurements with a sensitivity and accuracy comparable to laboratory equipment.

### 1.3.1 Field Methods

The SGLS utilizes a cryogenically cooled high-purity germanium detector and 4096-channel analyzer to obtain highly detailed gamma-ray spectra with energy resolution of a few kilo-electron volts. This approach provides in-situ measurements of gamma radioactivity that are comparable to laboratory measurements. Spectra are collected in "move-stop-acquire" mode where the sonde is held stationary for measurement and then moved a specified depth increment to the next measurement point. System gain is adjusted as necessary to maintain a consistent channel relationship for a marker peak (typically the $^{40}$K peak at 1461 keV). Verification measurements are made at the beginning and end of each logging day to assess system performance and to provide on-going energy and resolution calibrations for spectral analysis.

The typical depth increment is 0.5 ft. Measurement times are selected to detect prominent gamma peaks associated with natural radionuclides ($^{40}$K, $^{238}$U, and $^{232}$Th). Depending on casing thickness, a measurement time of 100 or 200 seconds (s) is generally used, resulting in logging speeds of feet per

hour instead of the feet per minute rates common in the petroleum and mineral industry. In deep boreholes with little or no contamination, a depth increment of 1.0 ft may be used to expedite logging. This larger depth increment is generally preferable to reducing count time, because the overall spectrum quality is not compromised.

### 1.3.2 Technical Methods

The peaks in the gamma energy spectrum correspond to gamma-ray photon energies characteristic of specific radioisotopes. The areas under the peaks are proportional to the gamma-ray flux intensities in the borehole, which are a function of the concentration of radioisotopes in the sediment surrounding the borehole. The spectrum includes peaks from the naturally occurring radionuclides $^{40}K$, $^{238}U$, and $^{232}Th$ and from the man-made contaminants $^{137}Cs$, $^{60}Co$, $^{152}Eu$ and $^{154}Eu$, antimony ($^{125}Sb$), and processed uranium ($^{235/238}U$). Gamma-ray source concentrations are cited in terms of picocuries per gram (pCi/g). This unit technically describes decay rate per unit mass of sample rather than concentration; however, the use of decay rate per unit mass is widespread in environmental work.

Gamma-ray energy spectra are processed to obtain the concentrations of individual gamma-ray-emitting radionuclides. The algorithms and equations applied in the peak evaluation and concentration calculations are discussed in the data analysis manual (manual in revision).

Log data and geological information from surrounding boreholes are assembled and correlated in an effort to identify contaminated zones and potential sources of contamination. Historical gross gamma, spectral gamma, and neutron log data are incorporated where available. Three-dimensional visualization software is used to interpolate data between boreholes.

A Waste Site Summary Report (WSSR) documents the results of the correlation and evaluation process for each group of waste sites. Waste site groups have been defined in terms of physical proximity and common configuration or operational history. Each WSSR provides a review of background information that includes a description and operational history of the waste sites, a summary of geologic and hydrogeologic conditions, a review of previous investigations, and any existing data such as gross gamma or spectral logs, geologic logs, or groundwater data. An assessment and interpretation of the spectral gamma-ray log information are also provided, along with conclusions and recommendations on future data needs or corrective action, where appropriate.

## 1.4 Project Objectives

Specific project objectives are:

- To use spectral gamma radiological methodology to identify the activities of man-made radionuclide contaminants and to estimate current subsurface radionuclide contamination in the vicinity of 200 Area waste sites. Many areas of the subsurface have been contaminated by the disposal of liquid waste to the ground, and, in some cases, by surface spills. The actual extent of the contamination is largely unknown, except for general information obtained from previous data collection activities and operational records.

- To identify probable sources of contamination by measuring the radionuclide contaminant activity in multiple boreholes and correlating data between those boreholes. It is possible, in many cases, to trace detected contamination back to probable sources.

- To provide a baseline dataset to help assess ongoing migration of the radionuclides through the vadose zone, and to provide data for the validation and initial or boundary conditions for contaminant transport models.

- To generate data that can be used for stratigraphic correlations in 200 Area waste sites. Migration of radionuclides through the vadose zone is affected by differences in composition, porosity, density, and water content. Accurate stratigraphic characterization helps in identifying target-monitoring horizons and in delineating controlling factors in subsurface flow. Lithologic characterization data include vertical profiles of naturally occurring $^{40}K$, $^{238}U$, and $^{232}Th$.

Although the primary focus of this project is interpretation and evaluation of spectral gamma logs, part of this project involves assessment of existing data, such as historical gross gamma data, spectral gamma and neutron logs, drilling logs, groundwater monitoring information, geology and hydrogeology information, construction details, and operational information. This information is compiled and evaluated with the newly acquired spectral gamma data to understand its significance in relation to the nature and extent of vadose zone contamination. The background and historical information helps to identify potential sources of contamination, the date of contamination, and to explain the nature of the contamination identified by the new spectral gamma log data.

# 2.0 Spectral Gamma-Ray Log Measurements

Existing boreholes are logged by the SGLS, which uses a cryogenically cooled HPGe detector with an intrinsic efficiency of approximately 35 percent. The HRLS is used in zones of high gamma activity, where the SGLS detector can become "saturated" and no usable spectra can be acquired. Both detector systems are operated on the same logging vehicle. Each combination of sonde and logging vehicle represents a unique logging system. Two logging vehicles, three SGLS sondes, and one HRLS sonde are available. Table 2-1 lists currently available logging systems.

Table 2-1. Logging Sondes and Vehicles (March 2002)

| | | | Vehicle | |
|---|---|---|---|---|
| **Sonde** | **Type** | **Serial No.** | **Gamma 1** HO 68B-3574 | **Gamma 2** HO 68B-3572 |
| A | SGLS | 34TP20893A | N/A[1] | (11/01)[2] |
| B | SGLS | 36TP21095A | N/A | (11/01) |
| C | HRLS | 39A314 | (11/02) | N/A |
| D | SGLS | 34TP11019B | (06/01) | N/A |

[1] Not applicable
[2] Date of last calibration

SGLS and HRLS log data are collected in accordance with a logging procedure (DOE 2001a). Gamma energy spectra are recorded at discrete depth increments. Typical count times are 100 or 200 s for the SGLS and 300 s for the HRLS. Verification spectra are collected at the beginning and

end of each logging day to monitor system performance, and repeat sections are logged to demonstrate repeatability and consistency.

Evaluation of gamma energy spectra provides identification and quantification of naturally occurring and man-made radionuclides on the basis of characteristic energy emissions associated with their decay. Only gamma rays of sufficient energy to penetrate the steel borehole casing and sonde housing can be detected by the SGLS or HRLS. Radionuclides that emit one or more gamma rays at energies between about 150 and 2,800 keV are detectable with the SGLS. The minimum detectable concentration is dependent upon detector efficiency at the appropriate energy, background activity, and the yield (gamma rays emitted, on average, per decay). Factors such as casing, water, shielding, and the presence of other radionuclides also have an effect. Because waste disposal to the soil column has been discontinued, radionuclides with half lives of less than one year have not been detected on the spectral gamma logs and are presumed to have decayed to insignificant levels. Tables 2-2 and 2-3 summarize naturally occurring and man-made radionuclides that can be detected with the SGLS. The terms "primary gamma ray" and "secondary gamma ray" are used to differentiate between the more prominent gamma energy peaks and other, less prominent peaks that may be useful for confirmation. The values indicated in bold are those generally used to calculate concentrations.

Table 2-2. Naturally Occurring Gamma-Emitting Radionuclides

| | **Primary Gamma Rays** | | | **Secondary Gamma Rays** | | |
|---|---|---|---|---|---|---|
| **Radionuclide** | **Daughter** | **E (keV)** | **Y (%)** | **Daughter** | **E (keV)** | **Y (%)** |
| $^{40}K$ | | **1460.83** | **10.67** | | | |
| $^{232}Th$ | $^{212}Pb$ | 238.63 | 43.30 | $^{228}Ac$ | 911.21 | 26.60 |
| | $^{208}Tl$ | **2614.53** | **35.64** | $^{228}Ac$ | 968.97 | 16.17 |
| | $^{208}Tl$ | 583.19 | 30.36 | $^{228}Ac$ | 338.32 | 11.25 |
| | | | | $^{208}Tl$ | 510.77 | 8.06 |
| $^{238}U$[1] | $^{214}Bi$ | **609.31** | **44.79** | $^{214}Pb$ | 295.21 | 18.50 |
| | $^{214}Pb$ | 351.92 | 35.80 | $^{214}Bi$ | 1120.29 | 14.80 |
| | $^{214}Bi$ | **1764.49** | **15.36** | $^{214}Pb$ | 241.98 | 7.50 |
| | | | | $^{214}Bi$ | 1238.11 | 5.86 |
| | | | | $^{214}Bi$ | 2204.21 | 4.86 |
| | | | | $^{214}Bi$ | 2447.86 | 1.50 |

[1] Attainment of secular equilibrium between $^{238}U$ and $^{214}Bi/^{214}Pb$ requires long time periods on the order of a million years. Activities of both $^{214}Bi$ and $^{214}Pb$ are commonly assumed to be equal to the activity of naturally occurring $^{238}U$. However, these radionuclides are short-term daughter products of $^{222}Rn$, and accumulations of radon gas inside the casing may temporarily elevate the decay activities of $^{214}Bi/^{214}Pb$ relative to the decay activity of $^{238}U$.

Table 2-3. Man-Made Radionuclides

| Radionuclide | Half Life (Years) | Primary Gamma Rays | | Secondary Gamma Rays | |
|---|---|---|---|---|---|
| | | E (keV) | Y (%) | E (keV) | Y (%) |
| $^{60}$Co | 5.2714 | **1332.50**<br>**1173.24** | **99.98**<br>**99.90** | | |
| $^{106}$Ru | 1.0238 | 511.86 | 20.40 | 621.93 | 9.93 |
| $^{125}$Sb | 2.7582 | **427.88** | **29.60** | 600.60<br>635.95<br>463.37 | 17.86<br>11.31<br>10.49 |
| $^{126}$Sn | 1.E+5 | **414.50** | **86.00** | 666.10<br>694.80 | 86.00<br>82.56 |
| $^{134}$Cs | 2.062 | 604.70 | 97.56 | 795.85 | 85.44 |
| $^{137}$Cs | 30.07 | **661.66** | **85.10** | | |
| $^{152}$Eu | 13.542 | **1408.01** | **20.87** | 121.78<br>344.28<br>964.13<br>1112.12<br>778.90 | 28.42<br>26.58<br>14.34<br>13.54<br>12.96 |
| $^{154}$Eu | 8.593 | **1274.44** | **35.19** | 123.07<br>723.31<br>1004.73<br>873.19 | 40.79<br>20.22<br>18.01<br>12.27 |
| $^{155}$Eu | 4.7611 | 105.31 | 21.15 | | |
| $^{235}$U | 7.038E+08 | **185.72** | **57.20** | 205.31 | 5.01 |
| $^{234m}$Pa ($^{238}$U[1]) | 4.47E+09 | **1001.03** | **0.84** | 811.00<br>766.36 | 0.51<br>0.29 |
| $^{237}$Np | 2.14E+06 | 312.17 | 38.60 | | |
| $^{238}$Pu | 87.7 | 99.853 | 0.0074 | 43.498 | 0.04 |
| $^{239}$Pu | 24110 | 129.30<br>**375.05**<br>413.71 | 0.0063<br>**0.0016**<br>0.0015 | | |
| $^{240}$Pu | 6563 | 104.234 | 0.007 | 45.244<br>160.308 | 0.045<br>0.0004 |
| $^{241}$Pu | 14.35 | 148.567 | 0.0002 | 103.68 | 0.0001 |
| $^{241}$Am | 432.2 | 59.54 | 35.90 | | |

[1] $^{234m}$Pa is a short-term daughter of $^{238}$U. Secular equilibrium is achieved relatively quickly. Because of the relatively low gamma yield, this peak is not observed when only background levels of naturally occurring $^{238}$U are present. Hence, the presence of gamma peaks associated with $^{234m}$Pa without corresponding peaks associated with $^{214}$Pb and $^{214}$Bi indicates the presence of chemically processed uranium.

Other radionuclides of interest, such as tritium ($^{3}$H), strontium-90 ($^{90}$Sr), and technetium-99 ($^{99}$Tc), are "pure" beta emitters and do not emit any gamma rays that can be detected with the SGLS. However, experience has shown that the presence of $^{90}$Sr at concentrations greater than about 1,000 pCi/g can be inferred from the *bremsstrahlung* generated from interaction of the high-energy beta emissions from $^{90}$Sr with the steel casing.

Field gamma spectra are processed and analyzed in accordance with a data analysis manual (manual in revision). Conventional gamma spectra analysis software is used to detect gamma energy peaks, identify the source radionuclide, and determine the net count rate, counting error, and minimum detectable activity. From the net count rate ($P_{n,}$ cps) for a specific energy peak, the apparent concentration of the source radionuclide ($C_a$ pCi/g) is determined by:

$$C_a = \frac{27.027}{Y} \times I(E) \times DTC \times K_c \times K_w \times K_s \times P_n ,$$

where Y is the radionuclide yield, I(E) is the logging system calibration function, DTC is the dead time correction, and $K_c$, $K_w$, and $K_s$ are energy-dependent correction factors for casing, water, and shielding. The calibration function, I(E), is unique for each combination of sonde and logging vehicle. Values of the calibration function are updated annually and documented in calibration certificates and a calibration report (Koizumi 2002). Concentration error and minimum detectable concentration are calculated using similar equations. The reported concentration error is based on only the estimated counting error. No effort is made to include the effects of errors in the calibration function or correction factors. These errors are discussed in the calibration report (Koizumi 2002). The term "apparent concentration" is used because the calibration model is based on an effectively infinite, homogeneous distribution uniformly distributed about the borehole axis.

Data are acquired with a typical counting time of about 100 s at each measurement position. The minimum detection level (MDL) of a radionuclide represents the lowest concentration at which the positive identification of a gamma-ray peak for that radionuclide is statistically defensible. A description of the MDL calculation is included in the data analysis manual (manual in revision).

For a counting time of 100 s, the MDL for $^{137}$Cs was typically about 0.2 pCi/g. The MDL differs slightly for each spectrum depending upon background activity and concentrations of other radionuclides at the data point. In regions of higher man-made radionuclide concentrations, the Compton background continuum becomes elevated, increasing the MDL value.

The MDL for $^{60}$Co was about 0.15 pCi/g; the MDL for $^{154}$Eu and $^{152}$Eu was about 0.2 pCi/g; and the MDL for $^{125}$Sb in the one borehole in which it was detected was less than 1 pCi/g. These values represent the lower limit of detection for the system when it is operated with a 100-s counting time.

Natural and man-made radionuclide concentrations, total gamma count rate, and dead time are plotted as a function of depth. These plots are included in a Log Data Report that also summarizes borehole construction details, logging conditions, analysis notes, and log plot notes, as well as a brief discussion of results and interpretations. When appropriate, comparison plots with other available logs are also included. Log Data Reports for boreholes in the study area are included in Appendix A on the accompanying CD-ROM. Waste Site Summary Reports such as this document integrate data and interpretations from the individual Log Data Reports to develop an understanding of subsurface conditions in the vicinity of the waste site.

# 3.0 Background and Physical Setting of the 216-B-35 to -42 Trenches

The information presented in the following sections was obtained from a variety of sources, including Waste Information Data System (WIDS), System Assessment Capability (SAC), DOE (1993a), Brodeur et al. (1993), Wood et al. (2000), the BX Tank Farm Report (DOE 1998a), and Horton and Randall (2000). The proximity of the 216-B-35 to -42 Trenches to nearby waste processing, storage, and disposal sites in the 200 East Area is shown on Figures 2 and 3.

## 3.1 Background of the 200 Areas

Established in 1943, the Hanford Site was originally designed, built, and operated to produce plutonium for nuclear weapons. Uranium metal billets were received in the 300 Area and fabricated into jacketed fuel rods. The fuel rods were loaded into graphite-moderated reactors in the 100 Areas. With the exception of 100-N, which also provided steam to the Hanford Generating Project, these reactors were operated for the sole purpose of producing $^{239}Pu$ from neutron activation of $^{238}U$. The fuel rods were then transported to the 200 Areas, where plutonium and uranium were separated from the residual activation and fission products using a variety of liquid chemical separation processes. The 600 Area includes portions of the Hanford Site not included in the 100, 200, or 300 Areas and served primarily as transportation corridors and buffer zones between the fabrication, irradiation, and chemical processing areas (DOE 1998b).

Chemical separations process facilities were sited in both the 200 East and 200 West Areas. The 200 North Area temporarily stored irradiated fuel rods, allowing certain short-lived fission products to decay before being shipped to separations plants. With the startup of the separation plants, high-level wastes containing the bulk of the fission products were discharged to large underground steel tanks, and large quantities of liquid wastes (primarily water) containing minor concentrations of radionuclides and chemicals were discharged to the soil column and percolated into the vadose zone. Depending on contaminant concentrations and a consequent need for isolation, liquid wastes were discharged either to surface ponds and ditches or to underground cribs, reverse wells, and French drains. These liquid disposal sites were located in the 200 Areas near the processing plants and in the nearby 600 Areas (DOE 1998b).

## 3.2 Geologic Conditions

This section summarizes the geologic setting of the Hanford Site and the 216-B-35 to -42 Trenches. Figure 4 shows the general stratigraphy for the B-BX-BY Waste Management Area, which includes the 216-B-35 to -42 Trenches. Lithologic information, used to develop stratigraphy, is the result of field analysis of sediment samples retrieved during borehole drilling operations and from nearby outcrops. When available, gross gamma-ray logs have been used to support the geologic interpretation. Most of the boreholes were drilled with a cable tool drill rig, and the samples were obtained from bailings, core barrels, or as retained cuttings, generally from 5-ft intervals. Lindsey and Law (1993), Lindsey et al. (1994), and Wood et al. (2000) presented detailed descriptions and interpretations of the geologic formations near and within the B-BX-BY Waste Management Area.

### 3.2.1 Stratigraphy

Overlying the basalt flows of the Columbia River Basalt Group are the Ringold Formation, the unnamed Plio-Pleistocene unit, the informal Hanford formation, and Holocene-Age deposits. Rockwell (1979), Reidel et al. (1992), Delaney et al. (1991), Lindsey (1991), Lindsey et al. (1994), and Bjornstad et al. (2002) (draft report) have presented extensive descriptions and discussions of these formations. Bjornstad et al. (2002) currently are formalizing the stratigraphic nomenclature for post-Ringold sediments at the Hanford Site. When the nomenclature proposed by Bjornstad et al. (2002) is finalized, it will be used in subsequent reports.

### 3.2.1.1 Columbia River Basalt Group

The Columbia River Basalt Group is comprised of 174,000 $km^3$ of tholeiitic flood-basalt flows that erupted between 17 and 6 million years ago and cover approximately 164,000 $km^2$ of eastern Washington, Oregon, and western Idaho (Reidel et al. 1989). The distribution of the basalt flows reflects the tectonic history of the area (Reidel et al. 1989). The basalt is as much as 4,000 m thick in the vicinity of the Hanford Site (Reidel et al. 1989; Glover 1985). The uppermost basalt flow, the Elephant Mountain Member, is at a depth of about 270 ft under the 216-B-35 to -42 Trenches (Rockwell 1979). Reidel et al. (1989), Reidel and Fecht (1981), and Rockwell (1979) presented additional information about the Columbia River Basalt Group.

### 3.2.1.2 Ringold Formation

Ringold sediments are predominantly comprised of layers of fluvial sand, ancient soils (paleosols), and lacustrine sand, silt, and clay (Lindsey 1996). This formation, as much as 600 ft thick across the Hanford Site, is comprised of uncemented to locally well-cemented clay, silt, fine- to coarse-grained sand, and pebble to cobble conglomerate. Ringold sediments are absent underneath the 216-B-35 to -42 Trenches (Williams et al. 2000). DOE (1993a) and other studies have identified the pre-Missoula gravel as Ringold.

### 3.2.1.3 Plio-Pleistocene Sediments

The Plio-Pleistocene unit sediments unconformably overlie the Ringold Formation. This unit is laterally discontinuous. Plio-Pleistocene sediments, which are absent in the vicinity of the 216-B-35 to -42 Trenches (Williams et al. 2000), are comprised of locally derived basaltic alluvium and pedogenic calcium-carbonate-rich material. Both of these facies may be present at some locations. The basaltic material is comprised of weathered and unweathered locally derived basaltic gravel containing varying amounts of sand and silt. The carbonate-rich sediments are comprised of calcium carbonate cemented silt, sand, and gravel interfingering with carbonate-poor sediments. The Plio-Pleistocene unit generally dips to the south-southwest. Bjornstad et al. (2002) have proposed naming these sediments the Cold Creek Interval.

In the past, the Plio-Pleistocene was divided into an upper silty sand to sandy silt designated as early Palouse soil and a lower calcium carbonate-rich interval often referred to as the "caliche layer" (Lindsey et al. 2000). Numerous investigations conducted in the 1990s have observed that the upper unit contains stratified fine sand indicative of lacustrine deposition and not eolian conditions associated with the early Palouse soil (Lindsey et al. 2000). The Plio-Pleistocene unit contains a series of old buried soil zones with calcium carbonate development indicative of an arid environment (Slate 1996).

The pre-Missoula gravel is comprised of quartzose to gneissic clast-supported pebble to cobble gravel with quartzo-feldspathic sand matrix that underlies the Hanford formation in the east-central region of the Cold Creek syncline and at the east end of Gable Mountain anticline east and south of the 200 East Area (Williams et al. 2000).

A compact, massive loess-like silt with minor fine-grained sand unit may overlie the Plio-Pleistocene unit. This unit is designated the "Early Palouse soil," and it can range to tens of feet thick. The Early Palouse sediments can grade upward into sediments similar to those at the base of the overlying Hanford formation, making the contact between these two lithologic units difficult to distinguish. The Early Palouse soil is thickest in the southwest and southeast portions of the 200 West Area, where it reaches a maximum thickness of 65 ft. The Early Palouse soil is not present underneath the 216-B-35 to -42 Trenches (Williams et al. 2000).

### 3.2.1.4 Hanford Formation

A series of Pleistocene catastrophic flood deposits, informally known as the Hanford formation, overlies the Plio-Pleistocene and older sediments throughout the Hanford Site. The Hanford formation is comprised of gravel, sand, and silt. The sediments of the Hanford formation are unconsolidated, uncemented, and highly transmissive for the flow of water. This formation is thickest in the central Hanford Site, where it thickens to 350 ft. The Hanford formation is divided into three facies (gravel-dominated, sand-dominated, and silt-dominated) that are gradational with each other. Bjornstad et al. (2002), Lindsey (1991), Reidel et al. (1992), and Wood et al. (2000) provide detailed discussions of the Hanford formation lithology. The Hanford Site is in the process of formalizing the stratigraphic nomenclature for the Hanford formation (Bjornstad et al. 2002).

Interpretations of sediment samples obtained from boreholes in the 200 Areas (Lindsey and Law 1993; Lindsey et al. 1994; and Reidel et al. 1992) have resulted in subdividing the Hanford formation into units (H1a, H1, H2, H2a, H3, and H4). Units H1a, H2a, H3, and H4 are laterally discontinuous, and H3 and H4 are locally identified at the base of the formation (Lindsey et al. 2000). These interpretations have placed the contact between the upper Hanford unit H1 and the intermediate Hanford unit H2 at depths of about 35 ft in the 216-B-35 to -42 Trenches. The Hanford H3 occurs at an approximate depth of about 220 ft underneath the 216-B-35 to -42 Trenches. Hanford H4 is absent.

The rhythmite facies sediments (Hanford H4) were deposited under slack water conditions and in back-flooded areas remote from the main flood channel. These sediments are comprised of thinly bedded, plane-laminated and ripple cross-laminated silt and fine- to coarse-grained sand and commonly display normally graded rhythmites a few centimeters to several tens of centimeters thick (Baker et al. 1991; DOE 1988b). This facies dominates the Hanford formation occurrence along the western, southern, and northern margins of the Pasco Basin, within and south of the 200 Areas.

The Hanford H3 unit varies from 40 to 50 ft thick, and this lower coarse-grained unit is comprised of pebble and cobble gravel with interbedded sand. The H3 generally consists of coarse-grained basaltic sand and granule to boulder gravel, and ranges from well sorted to poorly sorted. In outcrop, these sediments display massive bedding, planar to low-angle bedding, and large-scale planar cross bedding. The gravel-dominated facies was deposited by high-energy floodwaters in or immediately adjacent to the main flood channel.

The Hanford H2 unit is about 180 ft thick in the area of the 216-B-35 to -42 Trenches and is comprised of sand-dominated facies with interbedded silt lenses (Lindsay and Law 1993; Lindsey et al. 1994). Some laterally discontinuous silt-rich interbeds are reported in this area, and these high-silt content zones may have higher moisture content and $CaCO_3$ content than the surrounding sand-dominated material. The depositional facies are discontinuous in both horizontal and vertical extents,

and little correlation between boreholes has been possible in terms of the minor differences between such features as the silty sand and sandy silt layers (Lindsay and Law 1993; Lindsey et al. 1994).

Unit H1 is dominated by coarse to granule sand and lesser pebble gravel formed from a complex interfingering of gravel and sand-dominated facies (Lindsay and Law 1993; Lindsey et al. 1994). The relative abundance of gravelly facies decreases from the northwest to the south. As gravel content decreases, unit H1 interfingers with the more sand-rich strata of unit H2.

Clastic dikes comprised of layers of silt, sand, and granule gravel crosscut the Hanford formation. These clastic dikes generally crosscut the bedding as alternating vertical to subvertical dikes, although they do locally parallel bedding. Clastic dikes also occur in the older sediments (Fecht et al. 1999).

#### 3.2.1.5 Holocene Surficial Deposits

Holocene surficial deposits are comprised of a mix of silt, sand, and gravel deposited by a combination of eolian and alluvial processes (DOE 1988b).

#### 3.2.1.6 Backfill

The backfill for the 216-B-35 to -42 Trenches was probably derived from the excavated upper Hanford and overlying Holocene surficial deposits that were used to cover the trenches after remediation of the area. Backfill material generally is comprised of very poorly sorted gravel, sand, and silt (Price and Fecht 1976).

### 3.2.2 Structure

The Hanford Site is located in the Pasco Basin, which is a physical and structural depression in the Columbia Plateau created by tectonic activity and folding of the Columbia River basalts. The structural framework of the Pasco Basin began developing before Columbia River Basalt Group volcanism (Reidel et al. 1994) and was an area of subsidence that accumulated thick deposits of sediments and volcanic rock. This pattern continued through Columbia River Basalt Group volcanism. Anticlinal ridges were growing under north-south compression. This compression resulted in a series of anticlinal ridges and synclinal valleys with a general east-west trend. The north-south compression and east-west extension have persisted from at least the middle Miocene to the present (Hooper and Camp 1981; Reidel 1984; Hooper and Conrey 1989; Reidel et al. 1989).

The geologic structure of the Pasco Basin area is dominated by a series of east-west-trending anticlines and synclines; the 200 Areas are situated on the north limb of the Cold Creek syncline. Anticlines to the north and south create topographic high areas (Gable Mountain and Rattlesnake Mountain, respectively) with outcropping basalt flows. The Hanford Site 200 Areas are situated on the northern limb of the Cold Creek syncline where bedrock dips to the south at an angle of approximately 5 degrees. Approximately 270 ft of sediments overlie the dipping basalt bedrock in the vicinity of the 216-B-35 to -42 Trenches.

## 3.3 Hydrology

Hartman (1999) and Narbutovskih (1998) described the hydrology of the Hanford Site and the B-BX-BY Waste Management Area (WMA). The top of the water table beneath the 216-B-35 to -42 Trenches is located at depths ranging from 250 to 275 ft (76 to 83.8 m) and is declining. The top of this unconfined aquifer is at an elevation of about 401 ft (122.2 m) and within the H3. The base of the unconfined aquifer is believed to be the top of the basalt. The 216-B-35 to -42 Trenches are located in a region of very low hydraulic gradient between the groundwater mound beneath B Pond, which is located east of the 200 East Area, and the eastward-moving groundwater from the 200 West Area (Caggiano 1996). Figure 5 shows a groundwater table map of the Hanford Site for October 1955.

Hydraulic properties have been determined by aquifer testing that was conducted in a number of boreholes in the 200 East Area. The transmissivity and hydraulic conductivity were determined by analyzing the results of the aquifer tests; Connelly et al. (1992) provided details of these tests. Data were acquired in boreholes 299-E33-28, 299-E33-29, and 299-E33-30, which are located about 600 ft (180 m) west of the 216-B-35 to -42 Trenches. Transmissivity ranged from greater than 51,000 to greater than 56,000 square feet per day ($ft^2/d$), and the hydraulic conductivity ranged between 5,100 to 5,600 feet per day (ft/d). Due to the relatively flat hydraulic gradient, the direction of groundwater flow in the uppermost aquifer in the 200 East Area is difficult to determine; however, groundwater flow in the vicinity is estimated to generally be westward at a rate of 0.04 to 0.08 meters per day (m/d) (PNNL 1998).

In June 1996, an assessment groundwater monitoring program was initiated for WMA-B-BX-BY when elevated specific conductance was measured in groundwater monitoring well 299-E33-32, which is downgradient from this WMA and directly east of the 216-B-35 to -42 Trenches. Elevated specific conductance resulted from increases in nitrate, chloride, sulfate, and sodium concentrations. The June 1996 sample confirmed elevated specific conductance that was initially measured in the February 1996 sampling of the monitoring well. $^{99}Tc$ and nitrate concentrations are increasing in monitoring wells 299-E33-31, 299-E33-32, and 299-E33-42 (see Figure 3), which are located between the 216-B-35 to -42 Trenches and WMA B-BX-BY.

Sediments in the vadose zone vary from open-framework gravels of the gravel-dominated facies and interbedded sand and silt of the silt-dominated facies of the Hanford formation to calcium-carbonate-rich deposits of the Plio-Pleistocene unit to cemented gravels of the Ringold Formation. These sediments are characterized by numerous lateral discontinuities, such as pinchouts and erosion truncations, and flow patterns are irregular. If clastic dikes are present, they may enhance vertical flow patterns.

## 3.4 Description of the 216-B-35 to -42 Trenches

The 216-B-35 through 216-B-42 Trenches (Figure 3), which are located approximately 200 ft (60 m) west of 241-BX Tank Farm, were designed to percolate waste liquid into the ground. Under the concept of "specific retention," the trenches were designed to utilize the moisture retention capacity of the vadose zone sediments. The intent was to limit the volume of liquid disposed to each trench to 10 percent of the soil volume between the bottom of the trench and the groundwater table. Each trench was 252 ft (77 m) long, 10 ft (3 m) wide, and 10 ft (3 m) deep. The side slopes of the excavations were at a ratio of 1.5:1. Trending east-west, they are unlined excavations that were used

for a short period of time (less than 1 year). Aboveground pipelines were removed and the trenches were backfilled when the waste disposal capacity was reached. Figure 6 is a photograph of the area that shows the present surface condition of the trenches.

A review of existing drawings for the "BX Trenches" in WIDS indicated a conflicting number of trenches. Although the area designated for the location of the trenches is the same on each of the drawings, the spacing between the trenches and the number of specific retention trenches on the west side of the 241-BX Tank Farm is in question. Drawings H-2-2431 (dated 10/6/57) and H-2-36443 (dated 6/3/53) show a total of eight trenches. Trenches 216-B-35 through 216-B-41 are in a row going south to north, with the 216-B-42 Trench being located west of Trench 216-B-35. Drawings H-2-37986 (dated 4/26/74) and H-2-44501, Sheet 141, (dated 9/22/83), show a total of 12 trenches. These drawings show 11 trenches in a south to north row, with the northernmost trenches being numbered 216-B-41A, B, C, and D, respectively. The 216-B-42 Trench is located west of the 216-B-35 Trench. After reviewing the discrepancy and comparing the drawings to two 1965 aerial photographs, it was concluded that there are most likely seven trenches in a south to north row and that the 216-B-41A, B, C, and D trenches were not installed. A GPR survey performed in January 2001 identified seven trenches and several liners on the north end. The liners appear to be pipes that may be sections of the overground pipeline.

## 3.5 Operational History

Waste streams were intentionally discharged to specific retention trenches during 1953 and 1954 to support the fuel separations operations in the 200 East and West Areas. On the basis of the volume of liquid disposed to the 216-B-35 and 216-B-38 through -42 Trenches, the calculated “Effluent Volume/Pore Volume” ranged from 0.2 to 0.3 (DOE 2000). The 216-B-37 Trench received the greatest volume of liquid and reached a calculated “Effluent Volume/Pore Volume” of 0.8; the 216-B-36 Trench reached 0.4 (DOE 2000).

The bismuth phosphate process was used at B Plant and T Plant to separate plutonium from irradiated fuel from 1944 through 1956. The first step in the process was to dissolve the metal coating from the fuel rods. The next step dissolved the uranium and extracted the plutonium. The uranium waste, also known as the metal waste stream, contained the bulk of the uranium and 90 percent of the fission products (mostly $^{137}Cs$ and $^{90}Sr$). The plutonium stream went through two additional decontamination cycles to purify it, producing the first- and second-cycle waste streams. The first-cycle waste stream contained approximately 10 percent of the long-lived fission products and 1 percent of the plutonium. The coating waste was combined with the first-cycle waste. The liquid waste from these processes was initially stored in the single-shell tanks in tank farms. By 1948, limited space in the tank farms resulted in a decision to discharge the second-cycle waste to cribs. In 1951, the 242-B and 242-T Evaporators began to concentrate the first-cycle waste to reduce the volume of waste stored in the tank farms. By 1953, the need for tank space resulted in the first-cycle waste that was being stored in the single-shell tanks to be discharged via aboveground pipelines to specific retention trenches.

The time in use, volume of waste, source, and type of waste for each retention trench are shown in Table 3-1; Table 3-2 shows an estimate of the amount of specific radionuclides discharged to the soil column. The 216-B-35, -36, -38, -39, -40, and -41 Trenches were in operation between December 1953 and December 1954. These trenches received first-cycle supernatant waste from the 221-B Building. The major radionuclides in the wastes were $^{137}Cs$, $^{90}Sr$, plutonium, and uranium.

The 216-B-37 Trench received waste from the bottom of the 242-B Waste Evaporator tank in 1954. Early in 1955, the 216-B-42 Trench received tri-butyl phosphate waste from the Uranium Recovery process.

Table 3-1. Summary of the Operational History for the 216-B-35 to -42 Trenches

| Trench | Time in Use | Mean Estimate of Volume ($m^3$) | Source | Type of Waste |
|---|---|---|---|---|
| 216-B-35 | 02/1954 – 03/1954 | 1,560 | 221-B Building | First-cycle supernatant |
| 216-B-36 | 03/1954 – 04/1954 | 1,940 | 221-B Building | First-cycle supernatant |
| 216-B-37 | 08/1954 | 4,330 | 242-B-42 Waste Evaporator | Evaporator bottoms from 242-B Evaporator |
| 216-B-38 | 07/1954 | 1,430 | 221-B Building | First-cycle supernatant |
| 216-B-39 | 12/1953 –11/1954 | 1,470 | 221-B Building | First-cycle supernatant |
| 216-B-40 | 04/1954 – 07/1954 | 1,640 | 221-B Building | First-cycle supernatant |
| 216-B-41 | 11/1954 | 1,440 | 221-B Building | First-cycle supernatant |
| 216-B-42 | 01/1955 – 02/1955 | 1,500 | 221-U Building | Scavenged tributyl phosphate; uranium recovery waste from U Plant. |
| References: | DOE (1993a) | Bergeron et al. (2001) | Waite (1991) | Waite (1991) |

Table 3-2. Summary of Median Radionuclide Release Estimates for the 216-B-35 to -42 Trenches from Simpson et al. (2001). Radionuclides are decayed to January 1, 1994.

| Trench | $^{137}$Cs (Median Estimate in Curies) | $^{90}$Sr (Median Estimate in Curies) | $^{60}$Co (Median Estimate in Curies) | $^{99}$Tc (Median Estimate in Curies) | U (Median Estimate in kg) | $^{239/240}$Pu (Median Estimate in Curies) |
|---|---|---|---|---|---|---|
| 216-B-35 | 394 | 26.3 | 0.0782 | 2.02 | 52.1 | 0.1698 |
| 216-B-36 | 489 | 32.5 | 0.0972 | 2.51 | 64.4 | 0.2117 |
| 216-B-37 | 66,400 | 87,100 | 0.807 | 25.5 | 4080 | 41.49 |
| 216-B-38 | 362 | 23.7 | 0.0717 | 1.84 | 48.0 | 0.1564 |
| 216-B-39 | 371 | 24.9 | 0.0735 | 1.90 | 49.6 | 0.1599 |
| 216-B-40 | 415 | 27.3 | 0.0821 | 2.11 | 54.4 | 0.1795 |
| 216-B-41 | 365 | 23.9 | 0.0722 | 1.86 | 47.9 | 0.1566 |
| 216-B-42 | 334 | 346 | $5.91 \times 10^{-5}$ | 7.21 | 81.5 | 0.5303 |
| Reference: | Simpson et al. (2001). Radionuclides are decayed to January 1, 1994. | | | | | |

## 3.6 Previous Investigations

Review and visual comparison of gross gamma log profiles over time have been useful to determine if contamination has moved downward or changed in intensity. Due to the poor spatial resolution of the data (1 ft) and depth registration errors, tabulation of the maximum spatial peak count rates and comparison of those count rates over time are not recommended. Small changes in the position of the borehole probe between loggings cause large variations in the spatial peak count rates. Only by qualitatively reviewing changing trends in the temporal data is it possible to identify actual changes in the formation contamination concentration.

Previous investigators have reported three intervals of gamma contamination: (1) a zone of surface $^{137}Cs$ contamination to a depth of about 10 ft; (2) a thick zone of $^{137}Cs$ contamination below the base of the trenches; and (3) a zone of $^{137}Cs$ and $^{60}Co$ contamination in the water table to the top of the basalt. This thick zone of $^{137}Cs$ contamination also can contain lesser amounts of other radionuclides. Geophysical logging of monitoring wells and boreholes was conducted as early as 1957 at the facilities related to B Plant operations. Several subsequent evaluations of the log data were performed, including Raymond and McGhan (1964) and Fecht et al. (1977), which are described in this section. DOE (1993a) provided comprehensive descriptions of these studies, a discussion of gross gamma logging methodology, and interpretations of the data. DOE (1993a) also presented an evaluation of individual waste units such as cribs, ponds, trenches, and ditches. Brodeur et al. (1993) provided summaries of several waste units that include waste discharge histories, plan views of the sites, and geophysical log data acquired in the monitoring boreholes. Horton and Randall (2000) did a limited investigation of selected waste sites in the 200 East Area.

Raymond and McGhan (1964) provided gross gamma logs from a scintillation probe and reported a zone of contamination from about 20 to 75 ft below ground surface in groundwater monitoring well 299-E33-8. The scintillation probe system used had a lower detection limit reported as about 3 pCi/cc ($Ru^{106}$ - $Rh^{106}$). Recorder chart data may have been transferred to logarithmic graph paper to account for required scale changes needed to accommodate wide variations in gamma activity encountered during logging, which made direct observation and interpretation somewhat difficult (Raymond and McGhan 1964).

Fecht et al. (1977) evaluated the historical gross gamma-ray logs acquired in the area and identified elevated gamma-ray activity from the ground surface to a depth of about 60 ft. No evidence led to the conclusion that the contamination was migrating vertically or horizontally in the vadose zone since it was first identified by the gross gamma ray logging; however, the activity associated with the contamination was decreasing over time (DOE 1993a). Elevated activity was observed in the groundwater beneath the 216-B-35 through -41 Trenches (Figure 7) in all three monitoring wells (299-E33-8, 299-E33-10, and 299-E33-21), but Fecht et al. (1977) indicated that no conclusive evidence was available to determine that the trenches were the source of the contamination. The 216-BY Cribs or 241-BY Tank Farm (located approximately 900 and 400 ft northeast of the 216-B-35 through -41 Trenches, respectively) were speculated as sources of the contamination (DOE 1993a). Gross gamma-ray logs from wells and boreholes associated with the 216-BY Cribs indicated contamination occurred throughout the depth extent of the crib monitoring wells and boreholes, indicating that waste from the cribs probably contributed to the groundwater contamination. Observations of the gross gamma-ray data acquired in several groundwater monitoring wells adjacent to the 216-B-35 through -41 Trenches indicated that contamination appeared to be migrating in a southerly direction in the unconfined aquifer along the top of the basalt (DOE 1993a).

Boreholes 299-E33-21 and 299-E33-290 were logged in 1992 using Westinghouse's (WHC's) Radionuclide Logging System (RLS) (Brodeur et al. 1993). Data were acquired in these boreholes at 6-in. intervals with counting times of either 50 or 35 s. On the basis of the log of 299-E33-21, Brodeur et al. (1993) concluded that $^{137}Cs$ released at the 216-B-36 Trench reached groundwater. $^{137}Cs$ contamination was detected from the ground surface to a depth of 279 ft, the total depth of the borehole. Maximum $^{137}Cs$ activity of more than 5,000 pCi/g was detected between 11 and 24 ft. $^{60}Co$ contamination was also detected between depths of 188 and 278 ft at less than 2 pCi/g. No

other man-made radionuclides were detected. The depth to groundwater at the time of logging was 261 ft. Borehole 299-E33-290 is a 50-ft-deep vadose monitoring borehole near the center of the 216-B-38 Trench. $^{137}$Cs contamination was detected in two zones: near the ground surface and at the bottom of the borehole. $^{137}$Cs concentrations exceeded 5,000 pCi/g at the bottom of the borehole. $^{60}$Co was the only other man-made radionuclide detected in the borehole, detected at depths between 31 and 41 ft at concentrations less than 1 pCi/g.

Horton and Randall (2000) reported that the majority of the $^{137}$Cs contamination below the trenches is located in sandy gravel overlying fine-grained sand within about 40 ft of the ground surface. This conclusion is based on RLS (RLS-1 and/or RLS-2) log data, collected by Waste Management Federal Services Northwest (WMFS-NW) in the late 1990s, from boreholes 299-E33-286, 299-E33-287, 299-E33-288, 299-E33-289, 299-E33-290, 299-E33-8, and 299-E33-10. $^{125}$Sb was detected in well 299-E33-8 in a thin interval at about 34 ft with a maximum activity of 2.5 pCi/g. In well 299-E33-10, the response of the gross gamma from 21 to 23 ft was much higher than expected from the relatively low level of $^{137}$Cs, indicating the possible presence of a strong beta emitter, such as $^{90}$Sr, or a source of $^{137}$Cs remote from the borehole. A moisture gauge was also used to log these boreholes, and the results were equivocal.

# 4.0 Logging Results in the Vicinity of the 216-B-35 to -42 Trenches

This section details the results of the spectral and high rate gamma-ray logging of the 216-B-35 through -42 Trenches. Log Data Reports for these boreholes (Appendix A on accompanying CD-ROM) were previously submitted and are also available on the Internet at http://www.gjo.doe.gov/programs/hanf/HTFVZ.html.

## 4.1 Boreholes and Wells Logged

Eleven vadose zone boreholes and three groundwater monitoring wells are associated with the 216-B-35 to -42 Trenches. All boreholes and monitoring wells were logged with the SGLS. Table 4-1 lists the boreholes and groundwater wells that were logged with the SGLS and the HRLS during this investigation. The boreholes and wells used in the vadose zone characterization efforts for the 216-B-35 to -42 Trenches are shown on Figure 3 and listed in Table 4-1. Appendix A contains the individual Log Data Reports and log plots for the boreholes and groundwater monitoring wells logged with the SGLS and HRLS.

Table 4-1. Boreholes and Groundwater Monitoring Wells Logged with the SGLS and HRLS During the Investigation of the 216-B-35 to -42 Trenches

| Borehole | Date Drilled | Drilling Method | Previous Logging | SGLS Maximum Depth Logged (ft btc[1]) | HRLS Interval (ft btc) |
|---|---|---|---|---|---|
| 299-E33-8 | Sept. 1953 | Cable Tool | GG[2] & RLS[3] | 258.5 | none |
| 299-E33-10 | Jan. 1955 | Cable Tool | GG & RLS | 288.5 | none |
| 299-E33-21 | Feb. 1957 | Cable Tool | GG & RLS | 284.5 | 11 to 42 |
| 299-E33-286 | August 1982 | Cable Tool | GG & RLS | 53 | 26.5 to 51.5 |
| 299-E33-287 | August 1982 | Cable Tool | GG & RLS | 52.5 | 26 to 52 |
| 299-E33-288 | August 1982 | Cable Tool | GG & RLS | 52 | 21 to 41 and 47 to 52 |
| 299-E33-289 | August 1982 | Cable Tool | GG & RLS | 51.5 | 17 to 33 |
| 299-E33-290 | August 1982 | Cable Tool | GG & RLS | 51.5 | 24 to 36 and 43 to 51.5 |
| C3104 | August 2001 | Cable Tool | none | 260 | 12 to 47 |
| C3340 | June 2001 | Push | none | 35 | 13.5 to 36 |
| C3341 | June 2001 | Push | none | 59.5 | 13.5 to 24 and 29 to 34 |
| C3342 | June 2001 | Push | none | 59.5 | 13.5 to 35 |
| C3343 | June 2001 | Push | none | 59.5 | none |
| C3344 | June 2001 | Push | none | 59.5 | none |

[1] Below top of casing
[2] Gross gamma or scintillation probe
[3] Radionuclide Logging System

## 4.2 Radionuclides Detected

Only $^{137}$Cs, $^{60}$Co, and $^{125}$Sb were detected in the vicinity of the 216-B-35 to -42 Trenches. $^{137}$Cs was detected in every well and borehole. $^{60}$Co was detected with activities near the MDL in seven of the 14 boreholes that were logged. $^{125}$Sb was detected only in groundwater well 299-E33-8 (Appendix A), located about 70 ft (21 m) north of the 216-B-41 Trench. $^{125}$Sb was detected at depths between 32 and 34 ft (TOC[1] reference) at activities ranging from near the MDL (1 pCi/g) to 2.5 pCi/g. $^{152}$Eu, $^{154}$Eu, $^{235}$U, and $^{238}$U were not detected in any of the the boreholes. $^{137}$Cs was also detected at depths of 24 and 25 ft in groundwater well 299-E33-10, located 215 ft (65 m) southwest of the 216-B-Trench, at an activity of about 0.6 pCi/g. These low-level $^{137}$Cs concentrations are insufficient to explain the observed increase in total gamma in this interval, suggesting the presence of either a remote gamma source or a strong beta emitter such as $^{90}$Sr.

### 4.2.1 $^{137}$Cs

$^{137}$Cs was detected in every borehole in the vicinity of the 216-B-35 to -42 Trenches. Figure 8 presents a three-dimensional sphere plot that provides an enhanced perspective of the contaminant distribution. The sphere plot shows the 0.5-ft assays recorded by the SGLS and HRLS as spheres that are colored and sized to show the relative $^{137}$Cs concentration and indicate spatial position at which the assays were acquired. As shown on Figure 8, three intervals of $^{137}$Cs contamination were identified: (1) 0.3 to 10 pCi/g within 12 ft of TOC or about 10 ft below ground surface; (2) 0.3 to $10^5$ pCi/g at depths between 10 and 70 ft; and (3) 0.3 to 3.5 pCi/g in a 22-ft zone immediately above the current intercepted groundwater table.

[1] Unless otherwise noted, TOC is the zero reference for all SGLS and HRLS logging depths.

In addition, $^{137}$Cs contamination was detected continuously from the ground surface to a depth of 245 ft in groundwater monitoring well 299-E33-21. $^{137}$Cs was detected near the MDL (about 0.3 pCi/g) at depths of 163.5 ft in well 299-E33-8 and 217.5 ft in borehole C3104.

High gamma-ray intensities due to $^{137}$Cs activity that "saturated" the SGLS (Table 4-1) were detected in all wells and boreholes (except boreholes C3343 and C3344) located within 40 ft of the 216-B-35 through -42 Trenches. Because the SGLS was unable to record spectra with distinct full energy peaks in these intervals, the intervals were subsequently logged with the HRLS (Table 4-1). The maximum detected $^{137}$Cs activity was approximately $2x10^5$ pCi/g in borehole C3342 at a depth of 16.5 ft in the 216-B-38 Trench. Activities greater than 1,000 pCi/g were generally detected between 12 and 55 ft, with the highest activities (greater than $10^5$ pCi/g) above 35-ft depth or about 23 ft below the bases of the trenches.

$^{137}$Cs contamination was detected a few feet above the current intercepted groundwater table in all of the groundwater monitoring wells (Figure 8). Activities ranged from 0.3 to 3.5 pCi/g in this interval, which extends about 25 ft above the current groundwater level. However, $^{137}$Cs was not detected at equivalent elevations (240 to 260 ft) in recently drilled vadose borehole C3104 (Figure 8). The deepest $^{137}$Cs concentrations were detected below the top of the groundwater at the bottom of well 299-E33-21, where a maximum activity of 45 pCi/g was detected at 280 ft.

### 4.2.2 $^{60}$Co

$^{60}$Co was detected in two widely separated depth intervals at activities ranging from the MDL to 0.6 pCi/g. Figure 9 is a three-dimensional sphere plot of the $^{60}$Co subsurface distribution that provides an enhanced perspective of the contaminant distribution. The sphere plot shows the 0.5-ft assays recorded by the SGLS as spheres that are colored and sized to show the relative $^{60}$Co concentration and indicate spatial position. $^{60}$Co was detected in the interval from 30 to 72 ft in all of the boreholes located northeast of a line defined by well 299-E33-21 and borehole C3142 at activities ranging from 0.1 to 0.6 pCi/g, except for borehole C3340, which did not extend below 35 ft. $^{60}$Co contamination was not detected in any borehole above about 30 ft. $^{60}$Co was usually detected with $^{137}$Cs between 30 and 60 ft, and generally alone deeper in the subsurface (60 to 72 ft). $^{60}$Co was detected in all of the groundwater wells at activities ranging from the MDL to 0.3 pCi/g at depths below the intercepted groundwater table. Both $^{60}$Co and $^{137}$Cs were detected below the groundwater only in groundwater monitoring well 299-E33-21. In addition, $^{60}$Co was observed in borehole C3104 at 115 ft with an activity of about 0.1 pCi/g. $^{60}$Co may also be present higher in the borehole but was not observed due to the high recorded dead time associated with high levels of $^{137}$Cs activity.

# 5.0 Interpretation of Results

This section details the method and results of an interpretation of the spectral gamma-ray logging of the 216-B-35 through -42 Trenches. This interpretation is based on the data collected for the Hanford 200 Areas Spectral Gamma Vadose Zone Baseline Characterization Project.

All SGLS and HRLS log data collected from the boreholes and wells surrounding the 216-B-35 to -42 Trenches were assembled and correlated in an effort to identify geophysical markers,

contaminated zones, potential contaminant sources, and to provide data for application of proposed geophysical markers. The data acquired from 14 boreholes (Table 4-1) were interpreted and correlated with existing geophysical and stratigraphic models for the surrounding area. The simplified stratigraphic model for the 216-B-35 to -42 Trenches was used as a starting point (Figure 4) to identify potential geophysical markers. The spectral gamma-ray logs for the naturally occurring isotopes ($^{40}$K, $^{238}$U, and $^{232}$Th) and total gamma logs for each borehole were compared and correlated with those from surrounding boreholes and checked for the presence of man-made radionuclides. After noting any influences of man-made radionuclides and changes in casing thickness on the spectral and total gamma logs, geophysical markers were identified. The purpose of this exercise is to identify and correlate sedimentary features between boreholes that may influence the migration of contaminants in the vadose zone. One east-west cross-section, one southwest-northeast cross-section, and two north-south cross-sections were constructed from spectral gamma logs collected within the study area.

The process of interpreting the log data is described in the data analysis manual (manual in revision). In addition, C Tech Development Corporation's Environmental Visualization System (EVS) was used to perform the geostatistical analysis, generate geologic maps, and to create visualizations. Visualizations generated by EVS were then selected for the report and exported to a graphics program for annotation and final presentation.

## 5.1 Geophysical Correlation

All SGLS log data collected from the boreholes and wells surrounding the 216-B-35 to -42 Trenches are shown on Cross Sections A-A' (Figure 10), B-B' (Figure 11), C-C' (Figure 12), and D-D' (Figure 13) and correlated with the existing geophysical control in the surrounding area (Cross Section D-D', Figure 13). Figure 3 shows the locations of these cross sections. In the absence of man-made radionuclides, gamma-ray log response is proportional to clay and silt abundance, thus indicating possible changes in lithology. The spectral gamma-ray and total gamma-ray logs are much more useful to interpret stratigraphy than the older gross gamma-ray logs (compare the logs from well 299-E33-10 with 299-E33-32 on Figure 13) because of better sensitivity to small changes in radioactivity. The larger variations in $^{40}$K content (about 5 pCi/g) appear to be correlatable between boreholes. $^{40}$K content is probably the most reliable stratigraphic indicator.

Cross Section A-A' (Figure 10) passes through the 216-B-38 Trench, and Cross Sections B-B' and C-C' (Figures 11 and 12, respectively) are perpendicular to the orientation of the trenches. These cross sections illustrate the variation in the $^{40}$K content of the Hanford formation in the 216-B-35 to -41 Trenches and the relationship (if any) between the trenches and local contaminant distribution. The interpretation shown in Cross Sections A-A' and B-B' (Figures 10 and 11, respectively) indicates that the increase in $^{40}$K content, which occurs at log depths ranging from 30 to 40 ft, occurs at its highest elevation at borehole C3342. Cross Sections B-B', C-C', and D-D' (Figures 11 to 13, respectively) indicate that the top of this increased $^{40}$K content has less relief in the north-south direction than the east-west direction. As shown on Cross Section C-C' (Figure 12), correlatable gamma-ray peaks are apparent at an elevation of about 445 ft (135 m) in the cross section's boreholes.

KUT variations can be used to identify major changes in Hanford formation lithology. The gravel facies known as the H1 is identified by a relatively low $^{40}$K concentration of about 13 pCi/g and lower total gamma reading. The sand facies known as the H2 is identified by a marked increase in

apparent $^{40}K$ concentrations to about 17 pCi/g and an increase in total gamma count rate. The base of the H2 is defined as the point where apparent $^{40}K$ concentrations and total gamma count rate decrease. The H3 generally contains coarser sediment than the H2 and has gamma-ray response similar to H1; it is identified by lower total gamma count rates and $^{40}K$ concentrations ranging from 10 to 15 pCi/g. The H3 unit may also have occasional increases in total gamma count rate and $^{232}Th$ concentration. Locally correlatable layers may exist within each of these units.

## 5.2 Development of the Visualizations

Visualizations were prepared to illustrate the extent of contamination within the three-dimensional space that constitutes the vadose zone in the vicinity of the 216-B-35 through -42 Trenches. Creating the visualizations required developing geostatistical models of the $^{137}Cs$ and $^{60}Co$ contaminant distributions and the stratigraphy. However, there are not enough data points within the study area to support development of a three-dimensional geostatistical model. Therefore, visualizations of contamination in the vicinity of the 216-B-35 through -42 Trenches are limited to three-dimensional "sphere plots," which show contamination as detected in boreholes relative to the locations of the trenches, and to two-dimensional visualizations along section lines where sufficient data points are available for extrapolation. Because $^{125}Sb$ was detected in only one borehole, it was eliminated from the visualizations. The contaminant models are considered empirical models because they are based on data obtained by measuring the $^{137}Cs$ and $^{60}Co$ concentrations at discrete points in the subsurface and extrapolating those values into the nearby subsurface volume. They are not conceptual models based on assumed waste disposal and contaminant transport mechanisms, and no effort was made to calculate hypothetical distributions using contaminant transport models.

The visualizations are intended to provide the reader with an understanding of how the gamma-emitting contaminants may be distributed in the vadose zone sediments. The visualizations can also provide an assessment of the extent to which operations have contributed to contaminant distribution and to define areas of concern that may be the subject of future comprehensive and qualitative characterizations.

### 5.2.1 Development of the Interpreted Data Set

The radionuclide concentration values derived from the SGLS and HRLS data reported in the Log Data Reports were placed in data files that defined the position of each data point and the nuclide-specific concentration for that point. These data files were revised to create an "Interpreted Data Set," and the visualizations are based on these revisions. The revisions consist of removing radionuclide concentrations that are not considered reflective of actual formation concentrations and collapsing the borehole 0.5-ft sample interval to a 2.5-ft sample interval. This "2.5-ft sample" is the average of five 0.5-ft samples every 2.5 ft, which reduces the total size of the interpreted data set and better balances the vertical and horizontal distributions of the data points.

The interpreted data set reflects interpretations of the distribution and nature of occurrence of the contaminants as determined from experience and familiarity with the distribution of contaminants in the course of reviewing many SGLS logs. Intervals removed from the data set are those judged to represent contamination on the outside of the casing resulting from "dragdown" during drilling, internal casing contamination from a variety of sources, or contamination that either appears to be localized to the borehole or that may be from a remote source, such as a buried pipeline. Shape factor analysis was not used because the casing thicknesses were variable and not consistent with the

6-in.-diameter, 0.28-in.-thick casing for which the technique was developed. Occurrences of $^{137}Cs$ and $^{60}Co$ (regardless of the concentrations) were not deleted when they appeared to be correlatable laterally between boreholes, or when they were continuous at depth with no other contamination higher in the borehole. The interpreted data set also differs from the log data in that it contains only one value for each point. Log run overlaps are eliminated, and SGLS data are replaced with HRLS data where appropriate. In well 299-E33-21, "spikes" in $^{137}Cs$ activity between 140 and 240 ft were removed. These increases are about 10 pCi/g in magnitude and may be related to the welded casing joints causing an apparent "dragdown" or internal casing contamination during drilling. The intervals of $^{137}Cs$ contamination that have been removed from the SGLS data are indicated in Table 5-1. No $^{60}Co$ concentration data were removed from any borehole. The resultant concentration data are collectively referred to as the interpreted data set.

Table 5-1. Summary of the Interpreted Data Set Used During the Investigation of the 216-B-35 to -42 Trenches

| Borehole | Date Drilled | Interval(s) Edited | Comment |
|---|---|---|---|
| 299-E33-8 | Sept. 1953 | None | Drilled before the trenches were in operation. Contaminated intervals are widely separated. |
| 299-E33-10 | Jan. 1955 | None | Drilled shortly before the 216-B-42 Trench was in operation. Concentrations are less than 1 pCi/g, and contaminated intervals are widely separated. |
| 299-E33-21 | Feb. 1957 | 140 to 240 ft | Drilled after the trenches were in operation. $^{137}Cs$ was detected essentially over the entire length of the borehole. Between 140 and 240 ft, increases in $^{137}Cs$ activity appear to occur at an interval of roughly 10 ft. These spike increases of about 10 pCi/g may be related to the welded casing joints and were removed. The lower levels of $^{137}Cs$ were retained. |
| 299-E33-286 | Aug. 1982 | None | Drilled after the trenches were in operation. $^{137}Cs$ concentrations exceed 1,000 pCi/g at total depth (53 ft). |
| 299-E33-287 | Aug. 1982 | None | Drilled after the trenches were in operation. $^{137}Cs$ concentrations nearly 1,000 pCi/g at total depth (52.5 ft). |
| 299-E33-288 | Aug. 1982 | None | Drilled after the trenches were in operation. $^{137}Cs$ concentrations nearly 10,000 pCi/g at total depth (52.0 ft). |
| 299-E33-289 | Aug. 1982 | None | Drilled after the trenches were in operation. $^{137}Cs$ concentrations exceed 100 pCi/g at total depth (51.5 ft). |
| 299-E33-290 | Aug. 1982 | None | Drilled after the trenches were in operation. $^{137}Cs$ concentrations nearly 10,000 pCi/g at total depth (51.5 ft). |
| C3104 | Aug. 2001 | None | Drilled after the trenches were in operation. Drilled by telescoping casing. $^{137}Cs$ concentrations exceed 100,000 pCi/g at 30 ft. First casing string ends at 58 ft, while $^{137}Cs$ contamination terminates at 61 ft and $^{60}Co$ terminates at 72 ft. |
| C3340 | Jun. 2001 | None | Drilled after the trenches were in operation. $^{137}Cs$ concentrations exceed 10,000 pCi/g at total depth (35 ft). |
| C3341 | Jun. 2001 | None | Drilled after the trenches were in operation. $^{137}Cs$ concentrations are only about 10 pCi/g at total depth (59.5 ft). |
| C3342 | Jun. 2001 | None | Drilled after the trenches were in operation. $^{137}Cs$ concentrations are only about 10 pCi/g at total depth (59.5 ft). |
| C3343 | Jun. 2001 | None | Drilled after the trenches were in operation. Radionuclides were not detected below 10 ft. |
| C3344 | Jun. 2001 | None | Drilled after the trenches were in operation. Radionuclides were not detected below 10 ft. |

### 5.2.2 Two-Dimensional Visualizations

The horizontal distribution of boreholes within the study area was not adequate for development of a three-dimensional geostatistical model. Although kriging algorithms can be used to extrapolate data, the uncertainty increases with distance from known points. Therefore, the kriging capability in EVS was only used to extrapolate in two dimensions along A-A' and B-B' (Figure 3). A subroutine in EVS was used to model the surfaces defined by the geophysical interpretation vertical planes or cross sections. The output was a data field that provided the framework for kriging of properties within each layer. This data field was passed with the radionuclide concentration data to an EVS subroutine that created a quadrilateral finite-element grid with kriged nodal values and output this data for viewing. The visualizations were constructed to include the highest and lowest node values in two-dimensional space. Because nodes were set up at all data sampling points, the horizontal extent of the model and the visualizations were governed by the positions of the boreholes. The model does not extrapolate beyond the extent of either the range value or the kriging extent. As a result, both the model and the visualizations can only extend to the maximum depth of the boreholes and the extent of the geostatistical range unless other deeper boreholes are nearby. Once this fence of concentrations was developed, visualizations of the estimated concentration of each radionuclide could be produced that resulted in a planar surface model of the contamination.

The EVS software is an "expert" system that automatically determines parameter settings for the geostatistical model and for the kriging operation. These settings were used as a starting point for refinement of the model. Parameters were initially calculated by the software and then refined to create the most representative models for the $^{137}Cs$ and $^{60}Co$ distributions.

The kriging software applied an "anisotropy ratio" that allowed the user to affect the way data are extrapolated. The anisotropy ratio applied a bias to horizontal distances over vertical distances. The program default is 10, which means that vertical distances were multiplied by a factor of 10 before the distance between the grid point and the data point was calculated. A data point 1 ft above or below the grid point will thus appear to be 10 times farther away than a data point 1 ft away at the same level, and correspondingly will have less influence on the grid point. The anisotropy "forces" the kriging algorithm to give more weight to data points at the same level.

For data points where contamination was not detected, a minimum value of 0.01 pCi/g was entered into the input dataset; this value was extrapolated to the grid points. Grid points with values less than 0.1 pCi/g were "clipped" from the visualization to prevent non-detects from affecting data extrapolation.

Trenches were visualized by creating solid rectangular three-dimensional surfaces at the locations of the trench centers. In regions between the trenches, the model is not affected by the insertion of the trenches for the visualization; therefore, a borehole directly across a trench or within a trench can have some influence on a node-point concentration calculation. Because a geostatistical model was used in the concentration estimation calculation, the closest boreholes will have the most influence, and the model will be close to the actual distribution, except for areas where there are few boreholes.

## 5.3 Subsurface Radionuclide Distribution

As noted in Section 4.0, $^{137}Cs$, $^{60}Co$, and $^{125}Sb$ were detected while logging in this area. The distribution of radionuclides in the subsurface can be grouped according to origin. The near-surface

contamination (within 10 ft of the ground surface) is generally low levels of $^{137}$Cs (less than 10 pCi/g) that are thought to have been caused by small surface spills during waste transfers. The near-surface contamination will not be discussed further. The radionuclides detected at depths between 10 and 72 ft ($^{137}$Cs, $^{60}$Co, and $^{125}$Sb) are the result of wastes discharged to the 216-B-35 to -42 Trenches. The $^{137}$Cs and $^{60}$Co contamination detected near and below the present groundwater table may be the result of contaminant breakthrough to groundwater near the 216-B-36 Trench, as indicated by the spectral gamma log of well 299-E33-21 (Brodeur et al. 1993). Possible alternative sources of these contaminants may have been the BY Cribs or the BY Tank Farm (Fecht et al. 1977). Radionuclides from the 216-B-37 Trench may have broken through to groundwater; the effluent volume/pore volume ratio for this trench was calculated to be about 0.84 (DOE 2000). This trench received an estimated 57,000 Curies of $^{137}$Cs and 75,000 Curies of $^{90}$Sr (Simpson et al. 2001).

### 5.3.1 Subsurface $^{137}$Cs Distribution

$^{137}$Cs was detected in every borehole near the 216-B-35 to -42 Trenches, and visualizations were prepared in the areas of greatest control. A two-dimensional visualization was constructed along the 216-B-38 Trench using the boreholes shown on Cross Section A-A' (Figure 10). The visualization along Cross Section A-A' (Figure 15) and the log data shown on Cross Section A-A' (Figure 10) demonstrate that the majority of the $^{137}$Cs contamination is located immediately beneath the eastern half of the 216-B-38 Trench in the silty sandy to sandy gravels of the H1 unit. $^{137}$Cs contamination was present below the base of the trench in every borehole; the highest concentrations were detected within about 15 ft below the base of the trench. The log of borehole C3341 (Figures 10 and 15) suggests that the H1/H2 contact has caused lateral spreading as concentrations rapidly decrease in the H1 unit and then increase near the top of the H2 unit. At groundwater monitoring well 299-E33-8, which is located about 53 ft (16 m) north of the eastern end of the 216-B-41 Trench, $^{137}$Cs was detected within the H2 unit with only minor near-surface contamination in the H1 unit, supporting the interpretation that lateral subsurface spreading of radionuclides has occurred in the H2 unit.

$^{137}$Cs was not detected below the base of the 216-B-38 Trench in the two boreholes (C3344 and C3343) west of C3342, where the H1/H2 surface is at a relative high. The effects of the north-south-trending high in the H2 on the deposition of the H1 may explain why $^{137}$Cs was not detected below the base of the backfill in the western half of the 216-B-38 Trench. By applying the analogous site approach, it can be postulated that wastes discharged in the 216-B-35 to -41 Trenches did not spread past about the center of the trenches. If this is the case, the specific retention capacity of each trench should be adjusted downward to account for the fact that the majority of the percolation occurred in the upstream half of the trench, implying that breakthrough to groundwater may have occurred at the 216-B-37 Trench, where waste volume reached almost 84 percent of the specific retention volume for the entire trench. The trenches were designed to use the moisture-retention capability of the soils to retain contaminants. Liquid disposed to specific retention facilities was to ideally be limited to 6 to 10 percent of the soil volume between the facility and the groundwater so that all liquid would be retained in the soils (Waite 1991).

A two-dimensional visualization was constructed perpendicular to the 216-B-38 Trench using the boreholes shown on Cross Section B-B' (Figure 11). The visualization along B-B' (Figure 15) and log data shown on Cross Section B-B' (Figure 11) also demonstrate that the majority of the $^{137}$Cs contamination is located in the silty sandy to sandy gravels of the H1 unit. The visualization of Cross Section B-B' (Figure 16) differs from A-A' (Figure 15) in that all the boreholes except C3342

are not located within a trench, and the highest $^{137}$Cs concentrations are near the H1/H2 interface in four out of six boreholes. Unlike Cross Section A-A', the highest concentrations were usually deeper than 15 ft below the base of the trench.

$^{137}$Cs contamination was detected a few feet above the current groundwater table in all of the groundwater monitoring wells (Figures 12 and 13). Activities ranged from 0.3 to 3.5 pCi/g in this interval, which extends about 25 ft above the current groundwater level. The deepest $^{137}$Cs concentrations were detected below the top of the groundwater at the bottom of well 299-E33-21, where a maximum activity of 45 pCi/g was encountered at 280 ft. $^{137}$Cs contamination was continuously detected from the ground surface to a log depth of 245 ft in well 299-E33-21, and Brodeur et al. (1993) concluded that breakthrough to groundwater had occurred. As discussed in Section 5.1.1, there are indications that at least some of the contamination may be related to dragdown or casing contamination (e.g., the $^{137}$Cs "spikes" at regular 10-ft intervals) in this borehole. The $^{137}$Cs detected near the groundwater table in well 299-E33-8 is most likely not due to dragdown, because the well was drilled before the trenches were in operation, and the zones of major $^{137}$Cs contamination are separated by about 150 ft of clean borehole.

### 5.3.2 Subsurface $^{60}$Co Distribution

$^{60}$Co is distributed in two intervals that are separated by at least 190 ft in depth. Activities have now decayed to trace amounts (0.1 to 0.6 pCi/g ) because of the relatively short half-life of $^{60}$Co (about 5.2 years). The $^{60}$Co contamination detected at depths between 30 to 72 ft probably resulted from discharges to the trenches. $^{60}$Co was detected below the present groundwater table in the three groundwater monitoring wells (299-E33-8, 299-E33-10, and 299-E33-21). The source of this $^{60}$Co is not known.

Cross Sections A-A', B-B', C-C', and D-D' (Figures 10 through 13, respectively) depict the distribution of $^{60}$Co in the subsurface. The upper interval of $^{60}$Co (depths between 30 and 72 ft of the surface) is interpreted as residing in the H2 unit. $^{60}$Co was detected in all of the boreholes located northeast of a line defined by 299-E33-21 and C3142, except for borehole C3340, which did not extend below 35 ft. $^{60}$Co was not detected in the H1 unit or above a depth of about 30 ft. $^{60}$Co was generally detected without $^{137}$Cs deeper in the H2 unit (60- to 72-ft depth). At depths near the groundwater table, $^{60}$Co was detected at activities ranging from 0.1 to 0.3 pCi/g. The $^{60}$Co in the aquifer resides near the top of the basalt in both H3 and Pre-Missoula Gravel. Both $^{60}$Co and $^{137}$Cs were detected below the groundwater only at well 299-E33-21. $^{137}$Cs was detected with $^{60}$Co only in the H2 or H3 units.

## 5.4 Comparison to Prior Gamma Logging

A comparison of the SGLS (data acquired for this report) and RLS logs (previously acquired data ) was made to determine if any significant changes in subsurface contaminant profiles have occurred. The boreholes with existing RLS logs are listed in Table 4-1, and these comparisons are detailed in the Log Data Reports included in Appendix A. At first, significant discrepancies were identified in two of the seven boreholes for which a comparison could be made. The $^{137}$Cs values from the RLS logs for boreholes 299-E33-288 and 299-E33-290 appeared to be too low. The total gamma logs appeared to agree reasonably well, taking into account the difference in detector efficiencies. This agreement suggested that the field data are reliable and that the log data had been improperly reduced or plotted. These discrepancies were resolved by corrections to the existing RLS log data.

Comparison log plots of spectral gamma data collected in the 1990s and by this project are included in Appendix A, where applicable. The historical data are decayed to the date of the latest SGLS or HRLS logging event in 2002. On the basis of these comparisons, the apparent concentrations for the man-made radionuclides show good agreement between the logging systems when the decayed concentrations are above the SGLS MDL. Other than radioactive decay, no significant changes in contaminant profile appear to have occurred in any of the boreholes over the time periods between log events (3 to 10 years). Because these logs were all collected well after discharges to the trenches had ceased, the observed contaminant distribution appears to have been established during or shortly after the time the trenches were in service and has largely stabilized over the intervening years.

The gross gamma logging is the best historical record of the vadose zone contamination around the waste sites. This instrumentation was designed to respond in a consistent manner over the years, making it possible to compare spatial and temporal differences in relative peak count-rate spatial integrals. Unfortunately, the boreholes in the 200 Areas were not as consistently logged as in the tank farms. An extensive library of gross gamma logs is available for many of the boreholes. Once the limitations of these data are well understood, the data can be useful for assessing the general history of the vadose zone contamination. These systems were effective for high activity but were not sensitive to lower radionuclide concentrations (less than about 10 pCi/g equivalent $^{137}Cs$). Data were presented as plots of the gross count rate in counts per minute (cpm) as a function of depth. Gross gamma logs were visually compared with previous data to determine, in a qualitative manner, if changes had occurred. No additional processing or analysis were completed on these data.

When the gross gamma logs for the groundwater monitoring wells (299-E33-8, 299-E33-21) presented in Raymond and McGhan (1964), Fecht et al. (1977), and Additon et al. (1978) are interpreted based on the results of the SGLS, significant gamma-emitting contamination was present below 230 ft as early as July 1957. Current logging results indicate that low levels of $^{137}Cs$ and $^{60}Co$ are present at depths near and below the current ground water level, and the apparent 2002 total gamma activity decreases when the tool is submersed in the groundwater at the bottom of the boreholes. As early as 1957, gross gamma activity at the bottom of these boreholes appears to markedly increase on a logrithimic scale. As shown on Figure 6, radionuclides were present in groundwater in well 299-E33-8 in 1968 and in well 299-E33-21 in 1976. This contamination appears to be migrating in a southerly direction in the unconfined aquifer along the top of the basalt (DOE 1993a).

Raymond and McGhan (1964) presented gross gamma profiles for well 299-E33-8 from log runs on 5/4/59 and 5/17/63 (Figure 16). These logs indicate that significant amounts of gamma-emitting contamination appear to start at a log depth of about 230 ft (70 m) in 1959 versus about 246 ft (75 m) in the later log run. Ledgerwood (1993) reported that the depth to water at well 299-E33-8 was about 215 ft (relative to ground surface in November 1989). It should be noted that the original logs were not reviewed in this study, and the logs depicted in Raymond and McGhan (1964) are assumed as being correct representations of the logging events. On the basis of the increase in gross gamma activity relative to the KUT background, the $^{137}Cs$ and $^{60}Co$ contamination detected below 227 ft in groundwater monitoring well 299-E33-8 are speculated to have been emplaced via groundwater prior to May 1959.

Gross gamma profiles for well 299-E33-21 from Additon et al. 1978 (Figure 17) and Fecht et al. (1977) (Appendix A) indicate that significant amounts of gamma-emitting contamination were present below 250 ft as early as July 1957. Figure 17 is a logging run acquired on 7/31/57 and

shows that the gamma flux at the bottom of the borehole is nearly as intense as at the base of the trench. It should be noted that the original log was not reviewed and that this reproduction has an apparent depth registration error. Fecht et al. (1977) presented log runs from 5/4/59, 5/17/63, 4/27/70, and 5/4/76. The gamma contamination appears to start at about 262 ft (80 m) in 1959 versus about 273 ft (83 m) in the later log runs. The original logs depicted in Fecht et al. (1977) were not reviewed and are assumed as being correct representations of the logging events. The logging run from 1957 (Figure 17) suggests that breakthough to groundwater may have occurred in this area.

When the gross gamma profiles for well 299-E33-21 presented in Raymond and McGhan (1964), Fecht et al. (1977), and Additon et al. (1978) are interpreted on the basis of SGLS results, the $^{60}$Co and $^{137}$Cs contamination detected at depth are speculated to have resulted from the combined discharges to the nearby trenches, (i.e., the 216-B-37 Trench), or transported in the groundwater to this location. The $^{60}$Co contamination is only detected below groundwater in this borehole. $^{137}$Cs contamination detected at depths below groundwater may also have been emplaced by groundwater or from higher in the subsurface as $^{137}$Cs was detected over the entire length of the borehole with the SGLS.

## 5.5 Supplemental Interpretation

The influence of stratigraphy upon the subsurface distribution of radionuclides near Hanford's waste sites was recognized at least as early as 1948 (Brown and Rupert 1948). Because a unified geologic model has not been established for the 200 East Area, the geologic interpretations presented in Williams et al. (2000) and Wood et al. (2000) were consolidated into a single geologic model (Figure 4) for the study area based upon the results of geophysical logging and correlation. The purpose of correlating the stratigraphic units was to evaluate and account for their effect on lateral spreading. "Stratification tends to increase spreading of liquids along bedding planes and along contacts between sedimentary units" (Fecht et al. 1977). The Log Data Reports in Appendix A were completed prior to the production of this report, and the stratigraphic interpretation included in this report represents a compilation of the stratigraphic interpretations supplied in each individual Log Data Report.

### 5.5.1 Stratigraphy and Geologic Mapping

The stratified nature of the Hanford Formation has been recognized by many investigators (Lindsey et al. 1992, 1994, and 2000; Reidel et al. 1992; Lindsey and Law 1993; and Bjornstad et al. 2002). The type log for the study area is at groundwater well 299-E33-10 (see Figure 3 for location and Figure 13 for log). The Hanford formation is divided into three distinct units: H1, H2, and H3 (Figure 4). The H1 is identified by its relatively low $^{40}$K concentration of about 13 pCi/g and lower total gamma reading. The H2 is identified by a marked increase in apparent $^{40}$K concentrations to about 17 pCi/g and an increase in total gamma count rate. The base of the H2 is defined as the point where apparent $^{40}$K concentrations and total gamma count rate decrease. The H3 generally contains coarser sediment than the H2 and has gamma-ray response similar to H1; it is identified by lower total gamma count rates and $^{40}$K concentrations ranging from 10 to 15 pCi/g. The H3 unit may also have occasional increases in total gamma count rate and $^{232}$Th concentration. Locally correlatable layers may exist within each of these units. An expanded logging suite (including gamma-gamma density, neutron moisture, and neutron capture logs) would provide additional data with which to differentiate subtle variations in stratigraphy, and further subdivision of the Hanford units should

become possible. Table 5-2 summarizes stratigraphic interpretations of the available logs in the study area.

Table 5-2. Summary of the Geologic Interpretation of Boreholes and Wells in the Area Surrounding the 216-B-35 to -42 Trenches

| Borehole | Reference Elevation | Backfill | H1 | H2 | H3 | Pre-Missoula Gravel | Top of Basalt | Groundwater Depth |
|---|---|---|---|---|---|---|---|---|
| 299-E33-10 | 677.0 | np[1] | 3 | 60 | 209 | 268 | 287 | 275.5 |
| 299-E33-117 | 653.6 | 0 | 46 | 55 | nr[2] | | | |
| 299-E33-124 | 653.4 | 0 | 45 | 55 | nr | | | |
| 299-E33-125 | 653.0 | 0 | 46 | 60 | nr | | | |
| 299-E33-127 | 653.0 | 0 | 46 | 59 | nr | | | |
| 299-E33-153 | 657.4 | 0 | np | 40 | nr | | | |
| 299-E33-154 | 658.2 | 0 | np | 40 | nr | | | |
| 299-E33-155 | 658.6 | 0 | np | 41 | nr | | | |
| 299-E33-156 | 657.6 | 0 | np | 40 | nr | | | |
| 299-E33-167 | 659.7 | 0 | np | 43 | nr | | | |
| 299-E33-169 | 660.3 | 0 | 40 | 45 | nr | | | |
| 299-E33-170 | 660.0 | 0 | 40 | 46 | nr | | | |
| 299-E33-171 | 659.3 | 0 | np | 42 | nr | | | |
| 299-E33-172 | 659.8 | 0 | np | 43 | nr | | | |
| 299-E33-173 | 658.9 | 0 | np | 41 | nr | | | |
| 299-E33-174 | 659.1 | 0 | np | 40 | nr | | | |
| 299-E33-175 | 659.0 | 0 | np | 41 | nr | | | |
| 299-E33-21 | 671.7 | 0 | 12 | 45 | 224 | np | 280 | 267 |
| 299-E33-232 | 657.4 | 0 | np | 40 | nr | | | |
| 299-E33-237 | 658.9 | 0 | np | 40 | nr | | | |
| 299-E33-254 | 653.3 | 0 | 46 | 59 | nr | | | |
| 299-E33-255 | 653.2 | 0 | 46 | 58 | nr | | | |
| 299-E33-28 | 667.8 | np | 2 | 64 | 212 | nr | | 266 |
| 299-E33-286 | 672.6 | 2 | 4 | 41 | nr | | | |
| 299-E33-287 | 670.2 | np | 3 | 40 | nr | | | |
| 299-E33-288 | 669.4 | np | 3 | 36 | nr | | | |
| 299-E33-289 | 667.7 | np | 2 | 34 | nr | | | |
| 299-E33-29 | 677.3 | np | 2 | 57 | 213 | 285 | 290 | 275.5 |
| 299-E33-290 | 666.2 | np | 2 | 33 | nr | | | |
| 299-E33-31 | 650.8 | np | 0 | 50 | 205 | np | 255.6 | 249 |
| 299-E33-32 | 663.3 | np | 0 | 40 | 225 | np | 273 | 261.7 |
| 299-E33-42 | 657.6 | np | 0 | 30 | 238 | np | 260 | 255.9 |
| 299-E33-43 | 666.0 | np | 0 | 45 | 225 | np | nr | 264.4 |
| 299-E33-65 | 656.6 | 0 | 30 | 55 | nr | | | |
| 299-E33-77 | 662.2 | 0 | 40 | 54 | nr | | | |
| 299-E33-78 | 660.1 | 0 | np | 43 | nr | | | |
| 299-E33-8 | 654.3 | np | 3 | 28 | 212 | np | 257 | 253 |
| 299-E33-92 | 659.9 | 0 | np | 43 | nr | | | |
| 299-E33-93 | 660.3 | 0 | np | 43 | nr | | | |
| C3104 | 664.7 | 0 | 8 | 31 | 220 | np/nr | nr | |
| C3340 | 664.5 | 0 | 10 | 30 | nr | | | |

Table 5-2. Summary of the Geologic Interpretation of Boreholes and Wells in the Area Surrounding the 216-B-35 to -42 Trenches

| Borehole | Reference Elevation | Backfill | H1 | H2 | H3 | Pre-Missoula Gravel | Top of Basalt | Groundwater Depth |
|---|---|---|---|---|---|---|---|---|
| C3341 | 665.1 | 0 | 10 | 30 | nr | | | |
| C3342 | 665.3 | 0 | 11 | 29 | nr | | | |
| C3343 | 665.8 | 0 | 10 | 35 | nr | | | |
| C3344 | 666.0 | 0 | 11 | 39 | nr | | | |

[1] Not present

[2] Not reached

Only three wells in the 216-B-35 to -42 Trenches completely penetrated the Hanford formation and reached the basalt. The pre-Missoula gravel is differentiated from the overlying Hanford by a decrease in total or gross gamma-ray and $^{40}K$ activity in the pre-Missoula gravel. While pre-Missoula gravels are present in well 299-E33-10 west of the 216-B-42 Trench, they are absent in well 299-E33-8 and may be absent in well 299-E33-21 and at the east end of the 216-B-35 to -41 Trenches.

The H3 unit (Figure 4) is widespread and correlatable throughout the study area. It dips to the northeast at an orientation that appears to be conformable with the H2 unit (Figure 13). The top of the H3 ranges in elevation from 468 ft in the southwest (299-E33-10) to 438 ft in the northeast (299-E33-32).

Cross Section A-A' (Figure 10) passes through the 216-B-38 Trench, and Cross Sections B-B' and C-C' (Figures 11 and 12, respectively) are perpendicular to the orientation of the trenches. These cross sections illustrate the stratigraphy of the Hanford formation in the 216-B-35 to -41 Trenches and the relationship (if any) between the trenches and local contaminant distribution. The interpretation shown in Cross Sections A-A' and B-B' (Figures 10 and 11, respectively) indicates that the stratified layers of the H2 are at their highest elevation at borehole C3342. Cross Sections B-B', C-C', and D-D' (Figures 11 to 13, respectively) indicate that the top of the H2 unit has less relief in the north-south direction than the east-west direction. As shown on Cross Section C-C' (Figure 12), correlatable gamma-ray peaks at the base of H2 unit are apparent at an elevation of about 445 ft (135 m).

The top of H2 unit was the only stratigraphic horizon for which there were a sufficient number of penetrations to permit areal mapping. The surface of the H2 (Figure 18) appears to contain a local relative high that trends north-south underneath the 216-B-35 to -41 Trenches. At the east end of 216-B-35 through -41 Trenches, the H2 dips to the east. The amount of dip is less than 4 degrees or about 15 ft of drop over 410 ft. The top of the H2 ranges in elevation from 635 ft near the center of the 216-B-38 Trench to 593 ft northwest of single-shell tank 241-BY-110 (BY Tank Farm). Boreholes, where a stratigraphic determination was not possible primarily due to $^{137}Cs$ contamination, are shown by "dashed lines" on the cross sections (Figures 10 through 13). In these areas, the stratigraphy was projected on the basis of the results from the nearby boreholes, drilling logs, and the assumption that a change in $^{137}Cs$ distribution would occur at the H1/H2 interface.

### 5.5.2 Stratigraphic Influence on Contaminant Distribution

The H1/H2 surface (Figure 18) is considered as a horizon that could encourage lateral spreading of contaminated liquids discharged through the trenches. "Stratification tends to increase spreading of liquids along bedding planes and along contacts between sedimentary units" (Fecht et al. 1977). The logs of borehole C3341 (Figures 12 and 14) and well 299-E33-8 (Figure 12) suggest that the H1/H2 contact has enhanced lateral spreading. $^{137}$Cs concentrations detected in borehole C3341 rapidly decrease below 16 ft in the H1 unit and then increase near the top of the H2 unit at a log depth of 30 ft. In well 299-E33-8, located 53 ft (16 m) north of the eastern end of the 216-B-41 Trench, $^{137}$Cs was detected in the H2 unit with only minor surface contamination in the H1 unit, supporting the interpretation that the H2 unit has facilitated the lateral spreading of contaminants in the subsurface, since the wastes were discharged into the H1 unit. Thus, the map of the H1/H2 surface (Figure 18) can be used to predict the dominant direction of the lateral spreading of contaminants and to suggest locations for additional characterization boreholes.

Cross Sections A-A', B-B', and C-C' show the vertical distribution of $^{137}$Cs contamination and its relationship to stratigraphy (Figures 10, 11, and 12, respectively). The wastes were discharged directly into the H1 unit, and the highest observed $^{137}$Cs concentrations from the trenches appear to occur within the H1. These liquids were driven downward by gravity, and the vertical percolation of liquids probably dominated in the H1.

When the results of the contaminant and geologic mapping (Figures 10 through 15) are considered collectively, several observations on the past movement of $^{137}$Cs and $^{60}$Co in the H1 and H2 sediments can be made. The dominant direction of lateral spreading of the radionuclides from the 216-B-35 to -38 Trenches was probably to the east or southeast, which is down dip. Wastes from the 216-B-39 to -41 Trenches were more apt to spread laterally to the northeast. Wastes from the 216-B-42 Trench should have spread to the west or southwest.

Because the actual extent of the vadose contamination is unknown, a ratio of lateral spreading to vertical migration cannot be determined. The RCRA groundwater monitoring wells (299-E33-31, 299-E33-32, 299-E33-42, and 299-E33-43) east of the trenches were not logged with a spectral gamma tool prior to the installation of bentonite seals to below 200 ft. Subsequently, low levels of gamma-ray-emitting radionuclides could exist in the sediments surrounding these wells, and these boreholes cannot be used to constrain the distribution of low levels of radionuclides in the subsurface.

## 5.6 Potential Uncertainties and Inaccuracies

The interpretations discussed above are subject to a relatively high degree of uncertainty because of the number and distribution of boreholes with respect to the waste sites; consequently, the extent of the vadose zone contamination is poorly controlled both vertically and horizontally. For example, the focus of characterization efforts has been on the 216-B-38 Trench, which has been adequately characterized. The western and vertical extents of contamination appear to be defined, but the eastward extent of contamination is not known.

Some of the boreholes are open at the bottom and the lower end of the sonde comes in direct contact with sediment or contaminated material that migrated down the inside of the borehole casing. As a result, the gamma rays emitted from these sediments and/or materials are not attenuated by the

casing, but a casing attenuation factor is applied to the log data during processing. Therefore, the reported apparent concentrations may be slightly high at the bottoms of the boreholes. $^{137}$Cs contamination at the bottoms of boreholes that was interpreted to have resulted from migration down the inside of the casing is removed from the data to prevent overestimation of these $^{137}$Cs occurrences.

The construction of most boreholes is documented in the form of drilling logs. Most of the drilling logs provide varying degrees of detail and description regarding the drilling operations, geologic descriptions of sediments penetrated by the drilling, and explanation of the construction configurations of the "as-built" boreholes. Geologic sample descriptions are subjective and the depth control can vary by as much as 5 ft. The drilling logs provide information regarding when and how the boreholes were drilled and document the occurrences of radiological contamination that were encountered during drilling. The calculated radionuclide concentrations reported on the logs depend upon the reported casing thickness.

During cable tool drilling, the possibility exists that a borehole wall will collapse along the "open hole" portion of the borehole, before the steel casing is driven into place. If formation material sloughs from the borehole wall into the borehole, the sloughed material will be removed with the drive barrel; however, a void is created in the borehole. Once the casing is driven into place, the void may remain behind the borehole casing. Voids behind the casing or a highly rugose borehole can create a pathway for migration of contaminants down the outside of the borehole casing.

Plugs or caps were put into the boreholes to keep dust, contaminants, and water out of the boreholes, but the caps are not watertight and were meant merely to keep objects from inadvertently falling into the boreholes. If flooding occurred at the ground surface, water and contaminated sediments could potentially migrate down the outside of the borehole casings. If a borehole cap is removed for a significant amount of time, contaminated sand or silt can be blown into the borehole and settle at the bottom of the hole where it is evident as slightly elevated activity at the bottom of the borehole.

# 6.0 Conclusions

Eleven vadose zone boreholes and three groundwater wells in and near the 216-B-35 through -42 Trenches were logged with the SGLSs, and gamma-emitting radionuclide concentration data were generated at 0.5-ft intervals. Where high gamma flux was encountered by the SGLS, intervals of 10 of these boreholes were logged with the HRLS. Logging results were used to create a baseline data set for this collection of waste sites. Log Data Reports, which include log plots, were prepared and published separately for each individual borehole. The Log Data Reports provide a history of borehole and put the SGLS log data into an appropriate format to be used for waste site remediation and monitoring.

Only $^{137}$Cs, $^{60}$Co, and $^{125}$Sb were detected while logging in this study area. $^{137}$Cs contamination was detected in every well and borehole. $^{60}$Co contamination was detected in seven of the 14 logged boreholes. $^{60}$Co was detected at the 216-B-36 and -38 Trenches and north of the 216-B-41 Trench in the interval from 30 to 72 ft at activities ranging from 0.1 to 0.6 pCi/g. At depths below the intercepted groundwater table, $^{60}$Co was detected at activities ranging from 0.1 to 0.3 pCi/g in all of the groundwater monitoring wells. $^{125}$Sb contamination was detected only in groundwater well

299-E33-8 at depths between 32 and 34 ft with activities ranging from 1 to 2.5 pCi/g. $^{152}$Eu, $^{154}$Eu, $^{235}$U, and $^{238}$U (except natural background $^{238}$U) were not detected in any of the boreholes.

Empirical $^{137}$Cs and $^{60}$Co contamination distribution models were created. These cross sections and models were used to create visualizations of the contamination distribution that were reviewed and interpreted in this report. The geostatistical software and the visualizations are powerful tools for use in the assessment and interpretation of borehole contamination data. The information relating to the contamination distribution beneath the 216-B-35 to -42 Trenches can now be used to implement a monitoring program, to provide input for risk assessment, and for site remediation.

The results of the geophysical interpretation are that changes in the $^{40}$K content appear to have a greater influence on the total gamma-ray logs than the other naturally occurring radionuclides, and the contact between Hanford H1 and H2 units is a potential spreading surface. The Hanford formation is divided into three distinct units: H1, H2, and H3, which can be recognized in gamma logs by variations in $^{40}$K concentration and total gamma activity. The H1 is identified by its relatively low $^{40}$K concentration of about 13 pCi/g and lower total gamma reading. The H2 is identified by a marked increase in apparent $^{40}$K concentrations to about 17 pCi/g and an increase in total gamma. The base of the H2 is defined when apparent $^{40}$K concentrations decrease and total gamma increases. The H3 is identified by lower readings on the total gamma logs and readings ranging from 10 to 15 pCi/g on the $^{40}$K logs with occasional increases in total gamma and $^{232}$Th. The H1/H2 surface was mapped to predict the direction of lateral migration in the vadose zone. The predominant direction of lateral spreading of the radionuclides from the 216-B-35 to -38 Trenches appears to be to the east or southeast, which is down dip. Wastes from the 216-B-39 to -41 Trenches were more apt to spread laterally to the northeast while wastes from the 216-B-42 Trench should have spread to the west or southwest.

Three typical intervals of $^{137}$Cs contamination were identified: (1) 0.3 to 10 pCi/g within 12 ft below TOC; (2) 0.3 to $10^5$ pCi/g at depths between 10 and 70 ft; and (3) 0.3 to 3.5 pCi/g in a 22-ft zone immediately above the current groundwater table. The near-surface contamination (within 12 ft below the TOC) appears to have originated from small surface spills that occurred during waste transfers to the trenches and between other facilities. High gamma-ray intensities ($^{137}$Cs activities greater than 1,000 pCi/g) were detected between the base of the trenches and at a depth of about 53 ft. The highest $^{137}$Cs concentrations in each of these boreholes are detected within about 15 ft below the base of the trench. The radionuclides detected at depths between 10 and 72 ft ($^{137}$Cs, $^{60}$Co, and $^{125}$Sb) originated from discharges to the trenches when the trenches were in operation as waste disposal sites. The majority of the $^{137}$Cs contamination appears to be located immediately beneath the trenches in the silty sandy to sandy gravels of the H1. $^{137}$Cs contamination was detected a few feet above the current groundwater table in all of the groundwater monitoring wells. $^{137}$Cs activities ranged from 0.3 to 3.5 pCi/g in the interval, which extends about 25 ft above the intercepted groundwater level. However, $^{137}$Cs was not detected at equivalent elevations in the recently drilled vadose borehole C3104 (240- to 260-ft log depth).

In conjunction with the recent SGLS logs, published historic gross gamma logs were reviewed, and groundwater in the area appears to have contained contaminants as early as 1957. On the basis of a spectral gamma log of well 299-E33-21 (Brodeur et al. 1993), the $^{137}$Cs and $^{60}$Co contamination detected near and below the present groundwater table may have been caused by breakthrough of contaminants to groundwater near the 216-B-36 Trench, or the source of the groundwater contaminants may have been the BY Cribs or BY Tank Farm (Fecht et al. 1977). In the western half

of the 216-B-38 Trench, the vadose zone below the base of the trench appears to have not been contaminated due to a relative high in the H1/H2 surface, which was identified by the apparent $^{40}K$ activities. Similar geologic conditions exist at the 216-B-35 to -41 Trenches, suggesting that wastes did not spread past the center of the trenches and that the specific retention capacity of these trenches should be adjusted downward. These conditions imply that breakthrough to groundwater probably occurred at the 216-B-37 Trench.

A comparison between the recently collected log data and spectral gamma data collected in the 1990s (seven boreholes) shows good agreement in apparent $^{60}Co$ and $^{137}Cs$ concentrations. Where comparisons could be made, no significant changes in contaminant profile appear to have occurred during the last 3 to 10 years.

Although questions remain about the true nature and extent of the $^{137}Cs$ and $^{60}Co$ contamination, a high-quality database has been established for the $^{137}Cs$ and $^{60}Co$ contamination distribution beneath the 216-B-35 to -42 Trenches. Future monitoring can be conducted to determine if the contamination is moving, where the contamination is going, and if additional sources are present.

Discussion of hydrologic information is presented to place the vadose zone contamination in the 216-B-35 to -42 Trenches in context with the B-BX-BY WMA and what is known about nearby contamination conditions. Inclusion of this information illustrates the need for additional vadose zone characterization data to directly evaluate the 216-B-35 to -42 Trenches as a source of the groundwater contamination. The limited depths of some of the vadose zone monitoring boreholes in the area leave a significant portion of the vadose zone uncharacterized, creating a data gap between the depth extent of the boreholes and the contamination in underlying groundwater.

# 7.0 Recommendations

The vadose zone characterization of the 216-B-35 to -42 Trenches was conducted to establish a baseline value for gamma radionuclide activities in vadose zone sediments surrounding these waste sites. This baseline can be used to compare with future monitoring data to determine if changes have occurred and to assess the rate and potential causes of the changes. The data from this characterization project can also be correlated and compared with information other than concentration data, such as moisture data. From that comparison, needs for additional work are recognized that may provide insight as to the environment within which the contamination exists.

A lack of documentation on historical logging in this area currently exists. Additional work is recommended to collect, catalog, digitize, assess, and analyze historical gross gamma logging results for this area. Some work on collecting historical logs has been performed and presented in various publications that present only a fraction of the logs and are usually little more than a collection of logs with limited analysis results. This work is recommended to be continued and expanded to include all past logging runs and should also include assessments of past movement of vadose zone contamination that would be invaluable to remediation decision makers.

This initial characterization of the 216-B-35 to -42 Trenches vadose zone has identified several areas where future characterization efforts should be concentrated. A major data gap exists with regard to contamination conditions in and around the 216-B-37 Trench. Evaluation of the tables in Section 3

indicates that the 216-B-38 Trench received about 9 percent of the total liquid volume and about 0.5 percent of the $^{137}Cs$ discharged to the trenches. Trench 216-B-37 received about 28 percent of the total liquid volume and about 96 percent of the $^{137}Cs$ discharged to the trenches. Unfortunately, no boreholes are located within this trench. The 216-B-37 Trench received the bulk of the waste, both in terms of volume and radionuclide content, and yet there are no boreholes within the trench. A characterization borehole should be drilled to groundwater near the eastern end of this trench. The extent to which $^{137}Cs$ and $^{60}Co$ contamination is concentrated in the eastern portion of the trenches should be determined for all trenches. Logs from boreholes in the vicinity of Trench 216-B-38 suggest that contamination is concentrated in the eastern half of the trench, near the inlet. Contamination also appears to have tended to spread eastward from the trenches, at least at Trench 216-B-38, based on the dip of the H2. A series of additional boreholes is recommended to be installed this area. Two boreholes should be installed to a depth of 100 ft, at locations 50 and 125 ft east of borehole C3340 and the 216-B-38 Trench, respectively. To define the extent of lateral spreading of contamination from the 216-B-41 Trench, boreholes should be installed to a depth of at least 100 ft near the inlet of this trench and between the inlet and groundwater monitoring well 299-E33-8. The most significant contamination observed in the 216-B-35 to -42 Trenches, in terms of contamination extent, occurs near well 299-E33-21 (located near an inlet to the 216-B-36 Trench) and may be related to the discharges to the 216-B-35, 216-B-36, and 216-B-37 Trenches. There is insufficient control to constrain the lateral extent or identify the origin of the $^{137}Cs$ and $^{60}Co$ contamination detected at the bottom of this borehole. Additional boreholes should be drilled to investigate this area.

Any additional vadose zone characterization should include sampling and laboratory analysis to determine the occurrence and concentrations of radionuclides and chemical contaminants that do not emit gamma radiation (e.g., $^{90}Sr$ and $^{99}Tc$), which includes many of the high-risk radionuclides as well as RCRA constituents. For example, determining the presence of $^{99}Tc$, which was detected in groundwater beneath the B-BX-BY WMA, may provide insight regarding the migration characteristics of some of the contaminants detected in this initial characterization. Knowledge of the occurrence and distribution of these contaminants is a basic data requirement for determination of long-term risks that are used to evaluate proposed remediation strategies and tank waste retrieval alternatives.

Although borehole geophysical methods do not provide a comprehensive characterization dataset, the methods are useful because they are cost effective and safe and because numerous existing boreholes allow access to the subsurface. Other borehole geophysical methods, such as neutron, neutron capture, passive neutron and gamma-density logging, are recommended for development and implementation at the Hanford Site to provide better characterization data. These techniques should become part of an overall vadose zone characterization plan that includes adequate quality assurance so that data acquisition and analyses are fully documented and reproducible.

Because moisture movement provides the most likely driving force for the migration of radionuclides, it is recommended that an enhancement in this project be implemented to log all the boreholes with an effective moisture logging sonde.

# Figures

The following section presents the figures cited in this report in the order in which they were presented.

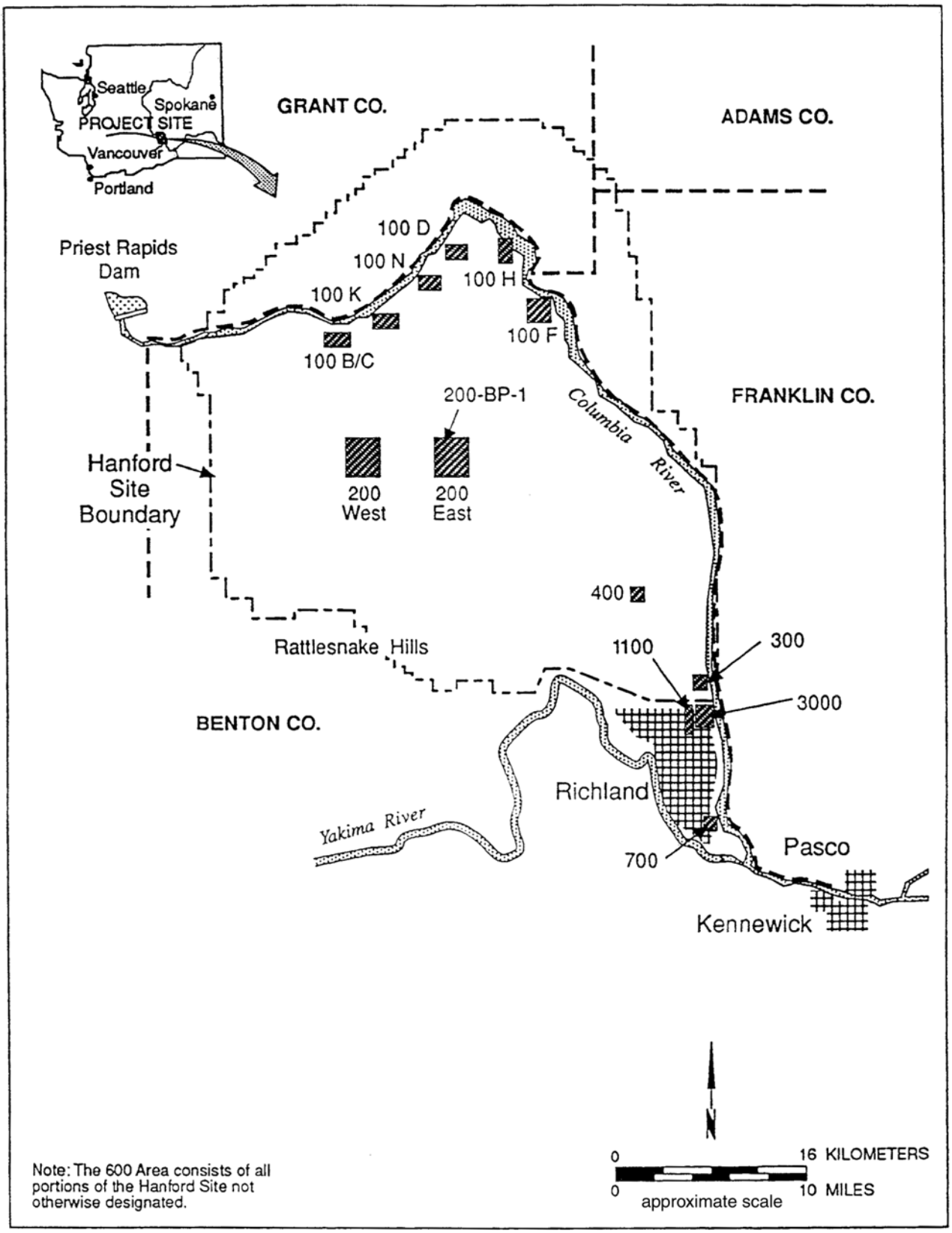


from DOE (1993b)

*Figure 1. Hanford Site and Area Designations*

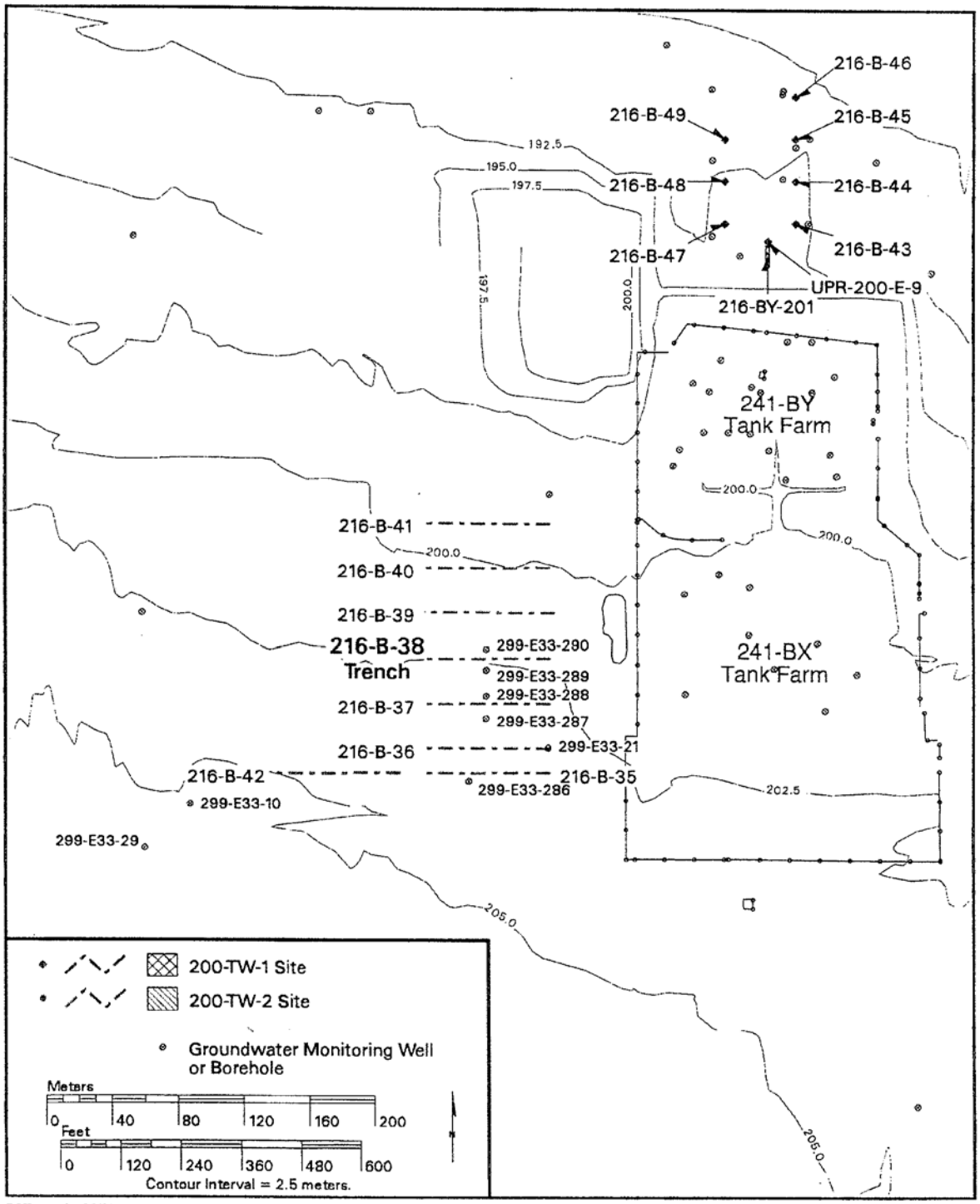


from DOE (2000)

*Figure 2. Map of the B-BX-BY Waste Management Area Showing the Proximity of 216-B-35 through -42 Trenches to Nearby Waste Processing, Storage, and Disposal Sites*

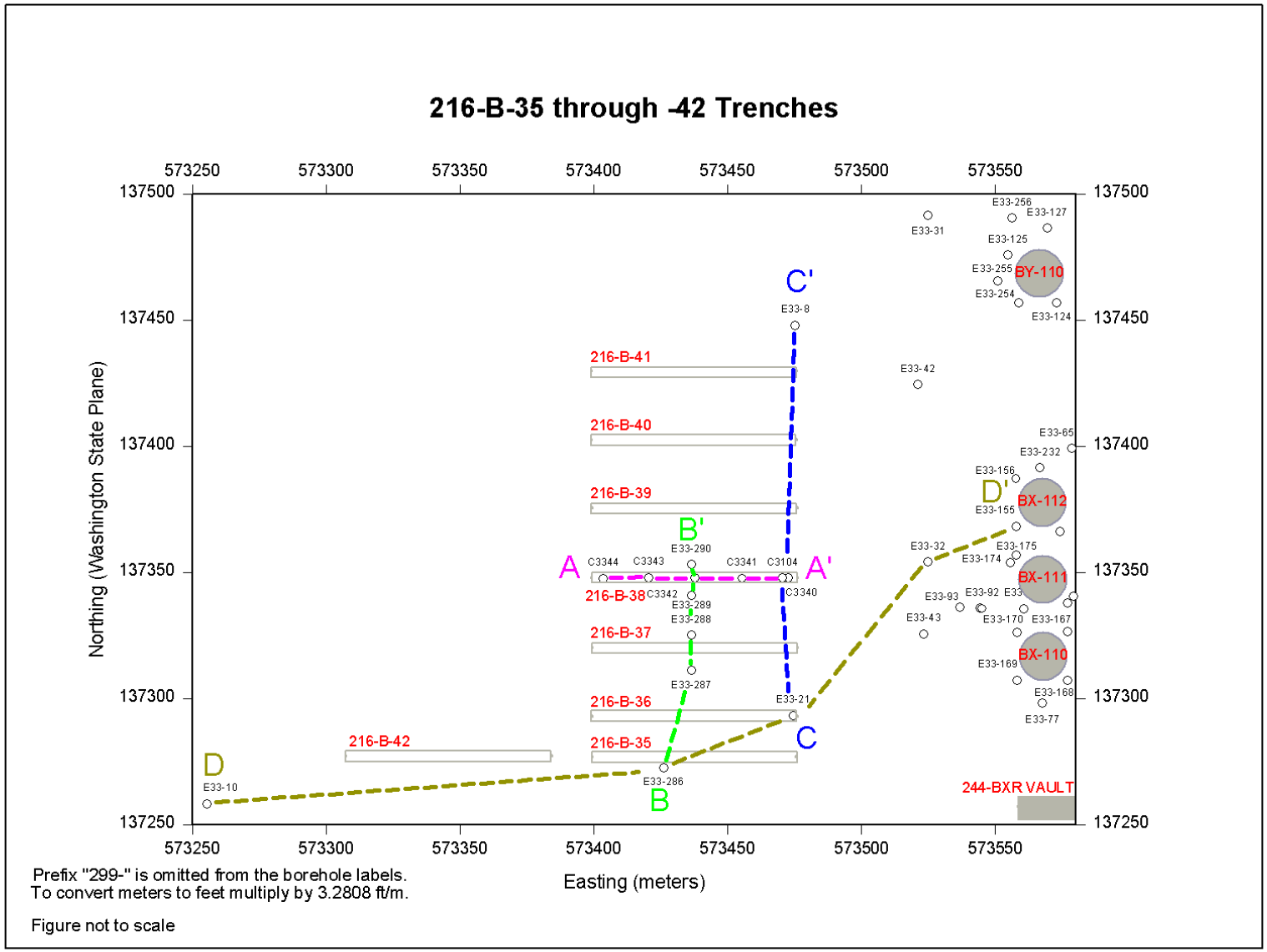


*Figure 3. Map of 216-B-35 through -42 Trenches Showing Locations of Waste Sites, Boreholes, and Cross Sections*

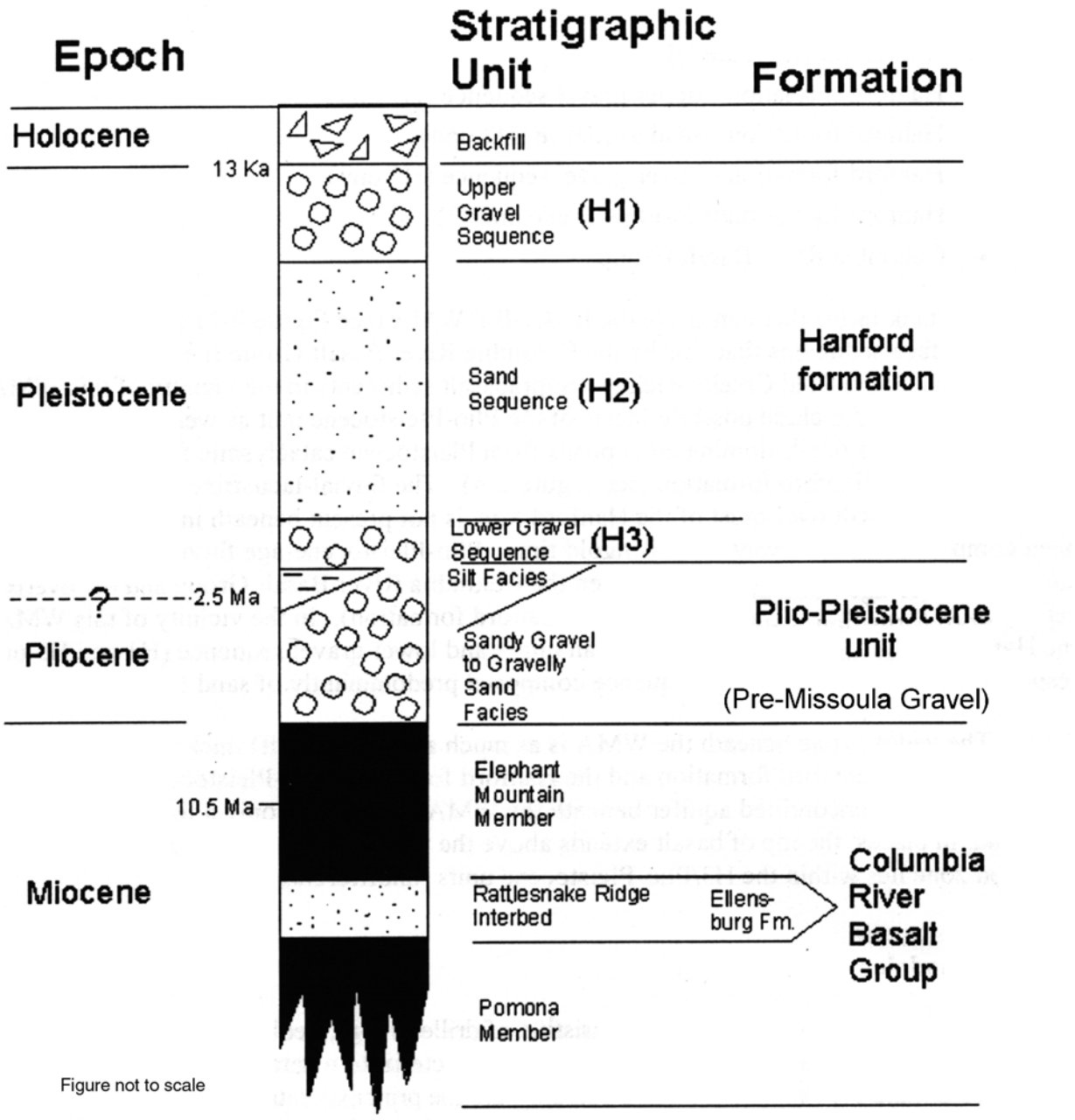


Modified from Wood et al. (2001)

*Figure 4. General Stratigraphy of the B-BX-BY Waste Management Area*

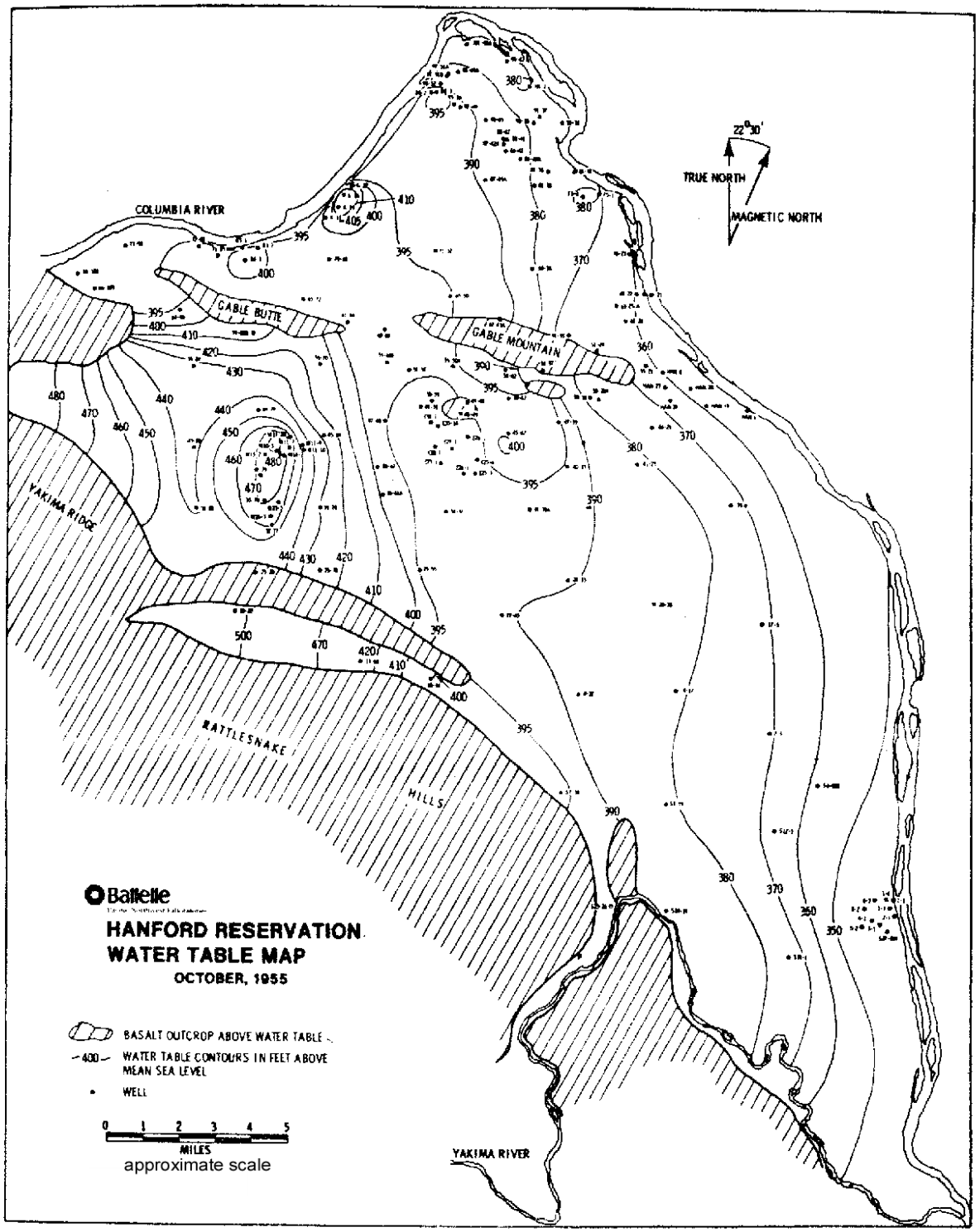


from PNL (1974)

*Figure 5. Groundwater Table Map of the Hanford Site for October 1955*

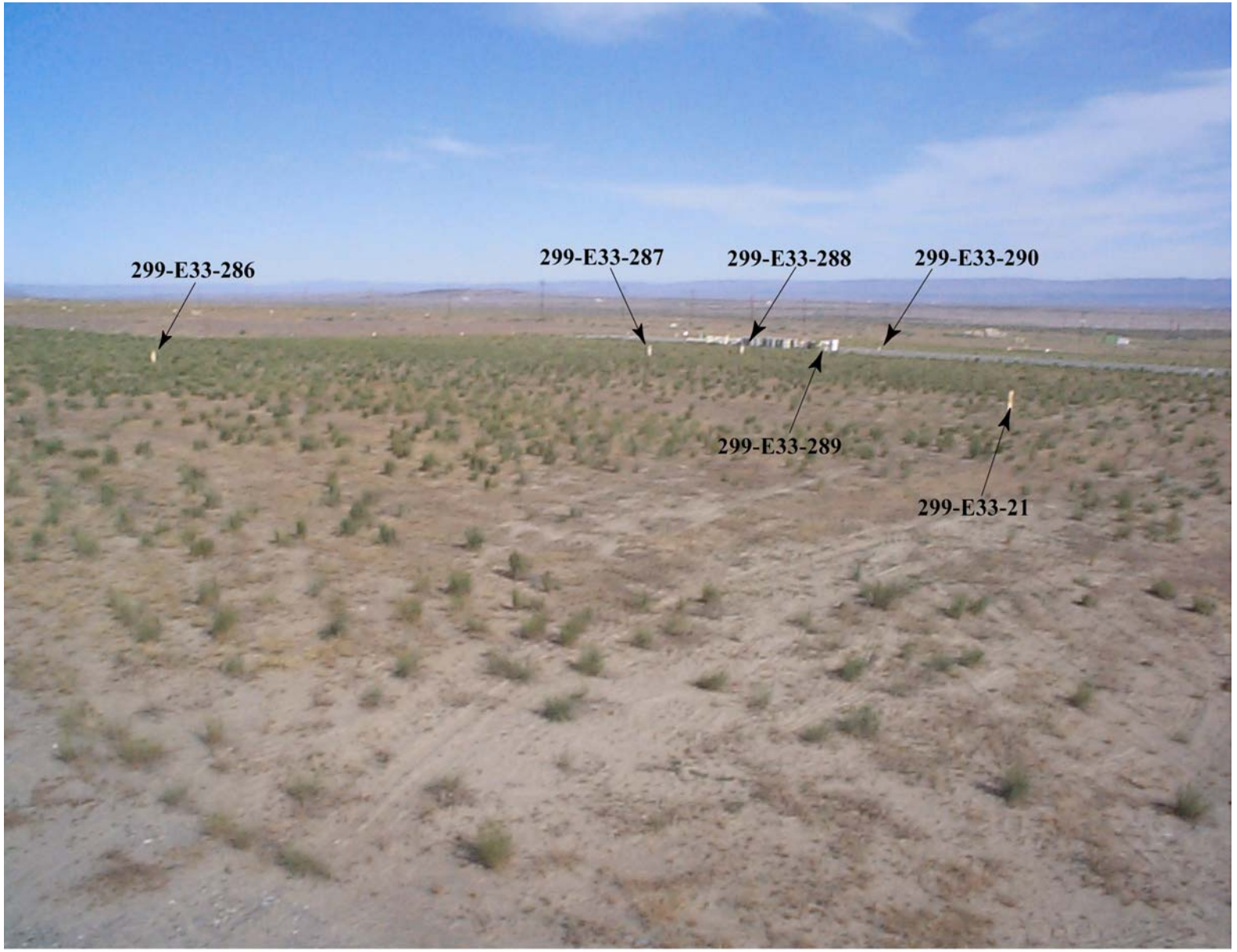


*Figure 6. Photograph of the 216-B-35 through -42 Trench Complex Viewed from the Southeast*

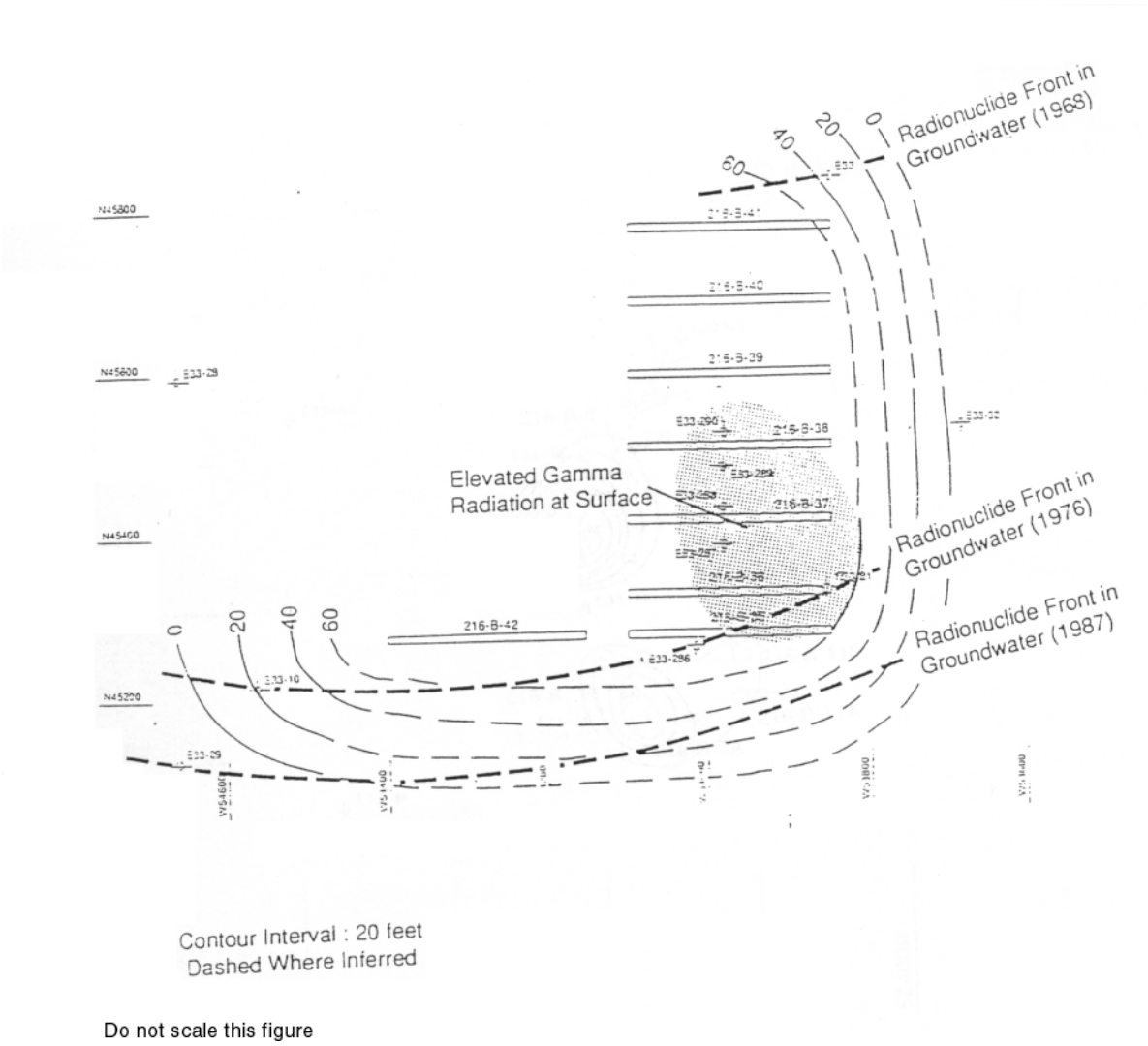


from DOE (1993b)

*Figure 7. 216-B-35 through -42 Trenches Elevated Gamma Radiation Isopach Map*

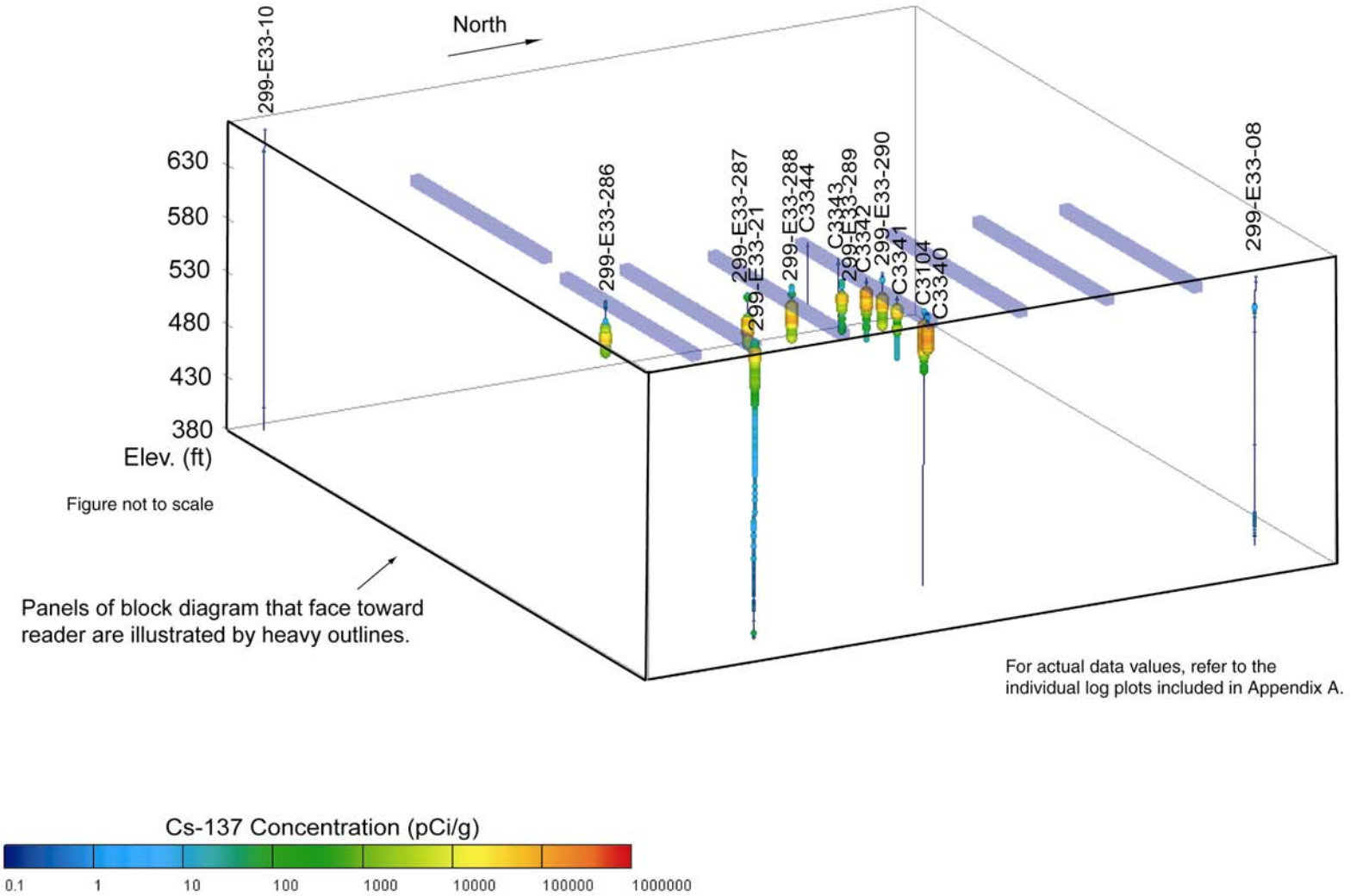


*Figure 8. Visualization of the Cs-137 Data Acquired at the 216-B-35 to -42 Trenches*

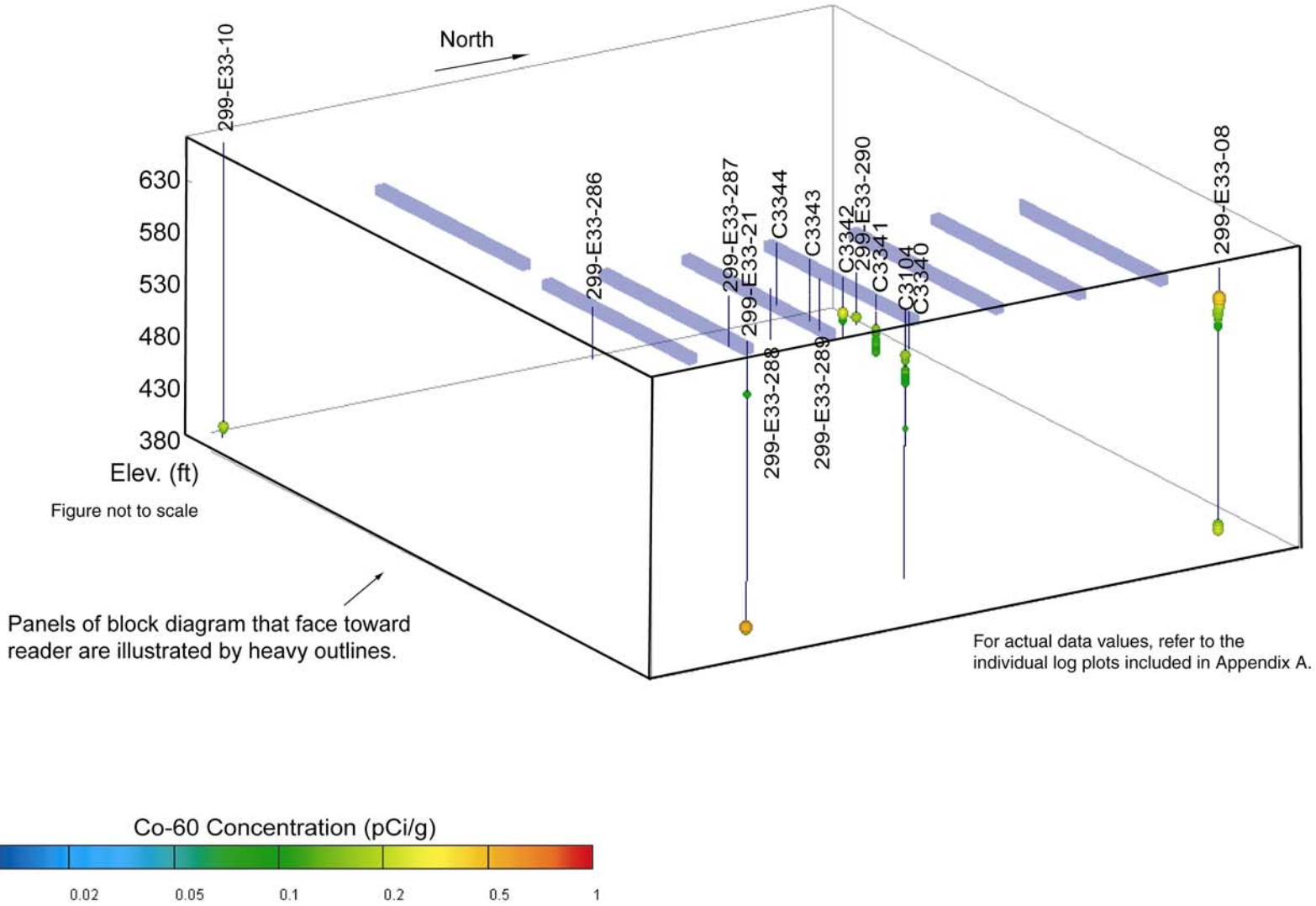


*Figure 9. Visualization of the Co-60 Data Acquired at the 216-B-35 to -42 Trenches*

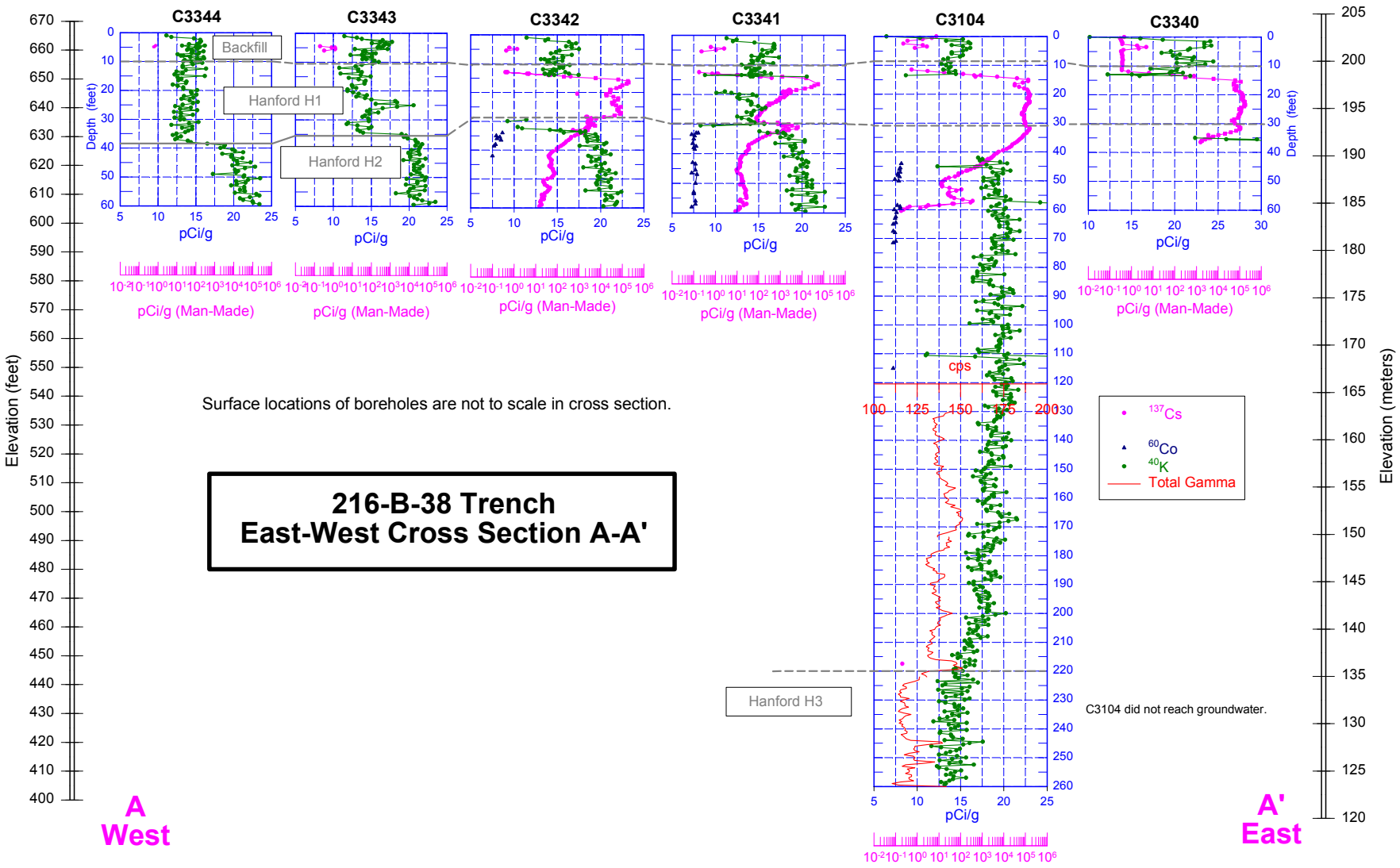


*Figure 10. Cross-Section A-A' Showing the Contamination and Interpreted Stratigraphy Along the 216-B-38 Trench*

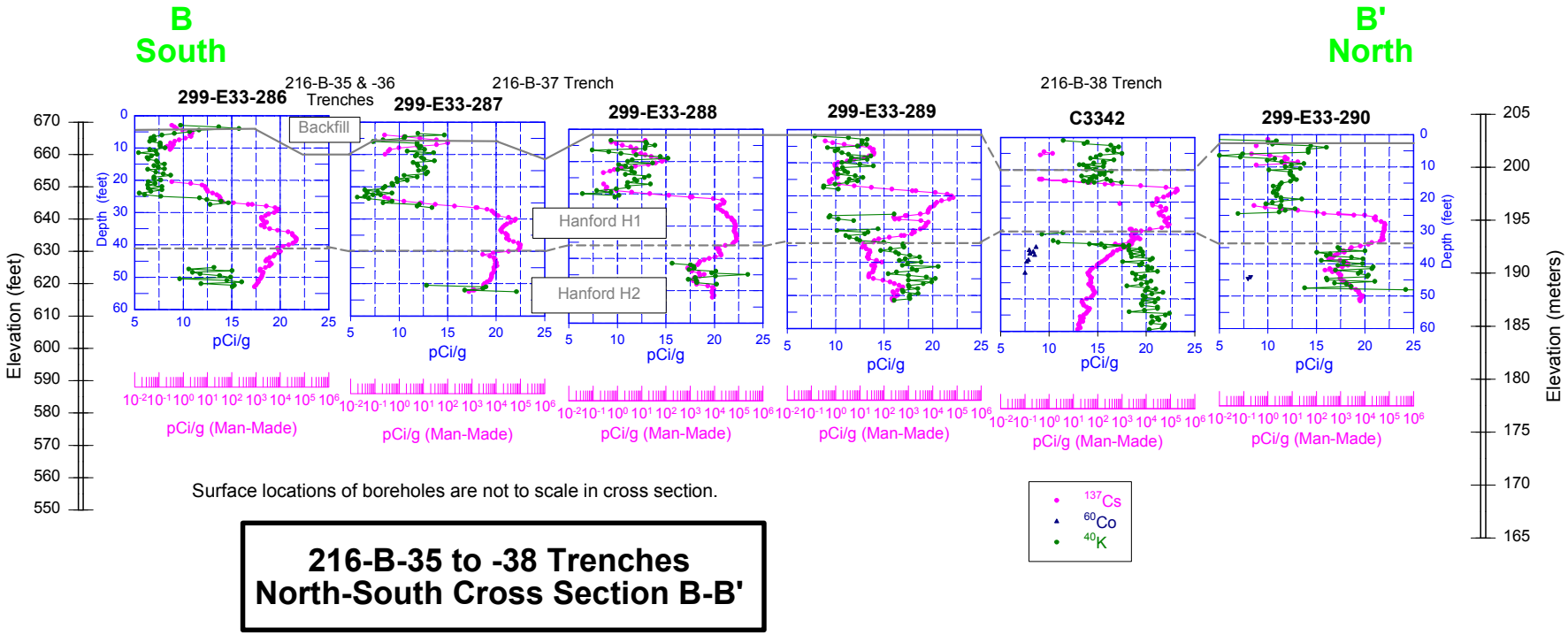


*Figure 11. Cross-Section B-B' Showing the Contamination and Interpreted Stratigraphy Perpendicular to the 216-B-35 to -38 Trenches*

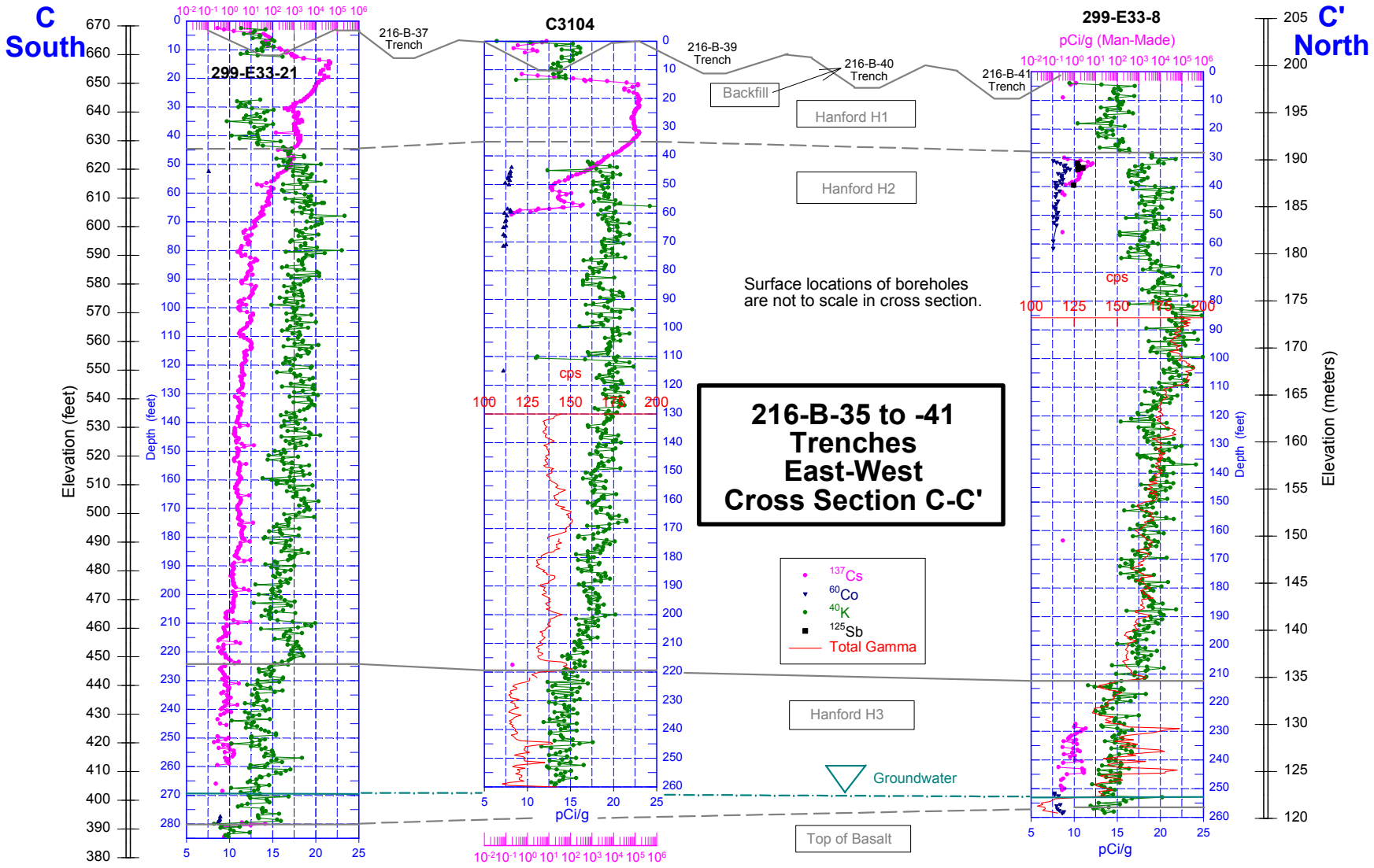


*Figure 12. Cross-Section C-C' Showing the Contamination and Interpreted Stratigraphy Perpendicular to the 216-B-35 to -38 Trenches*

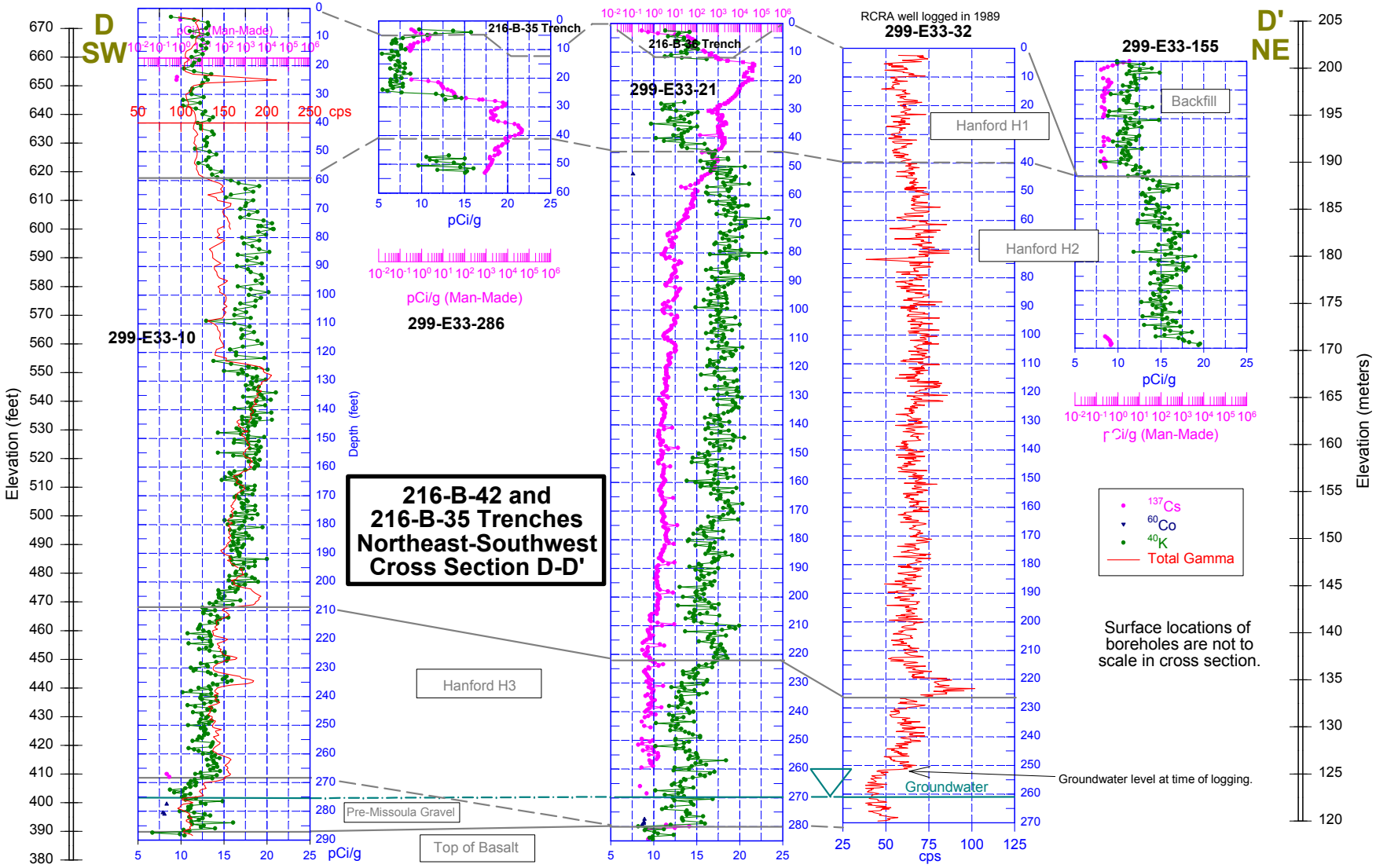


*Figure 13. Cross-Section D-D' Showing the Contamination and Interpreted Stratigraphy Perpendicular to the 216-B-35 to -41 Trenches*

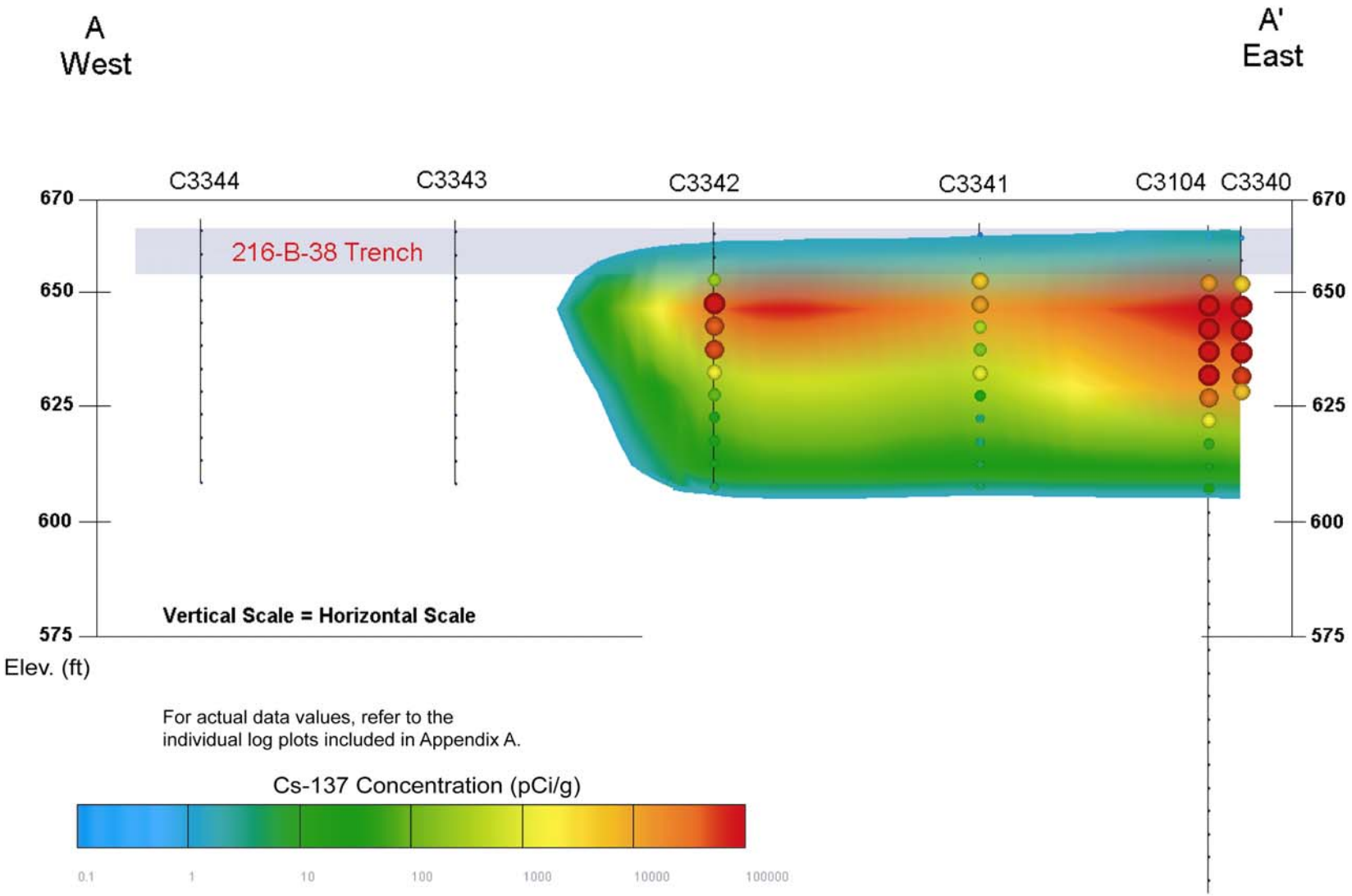


*Figure 14. Visualization of Cross-Section A-A' Showing the Cs-137 Contamination Along the 216-B-38 Trench*

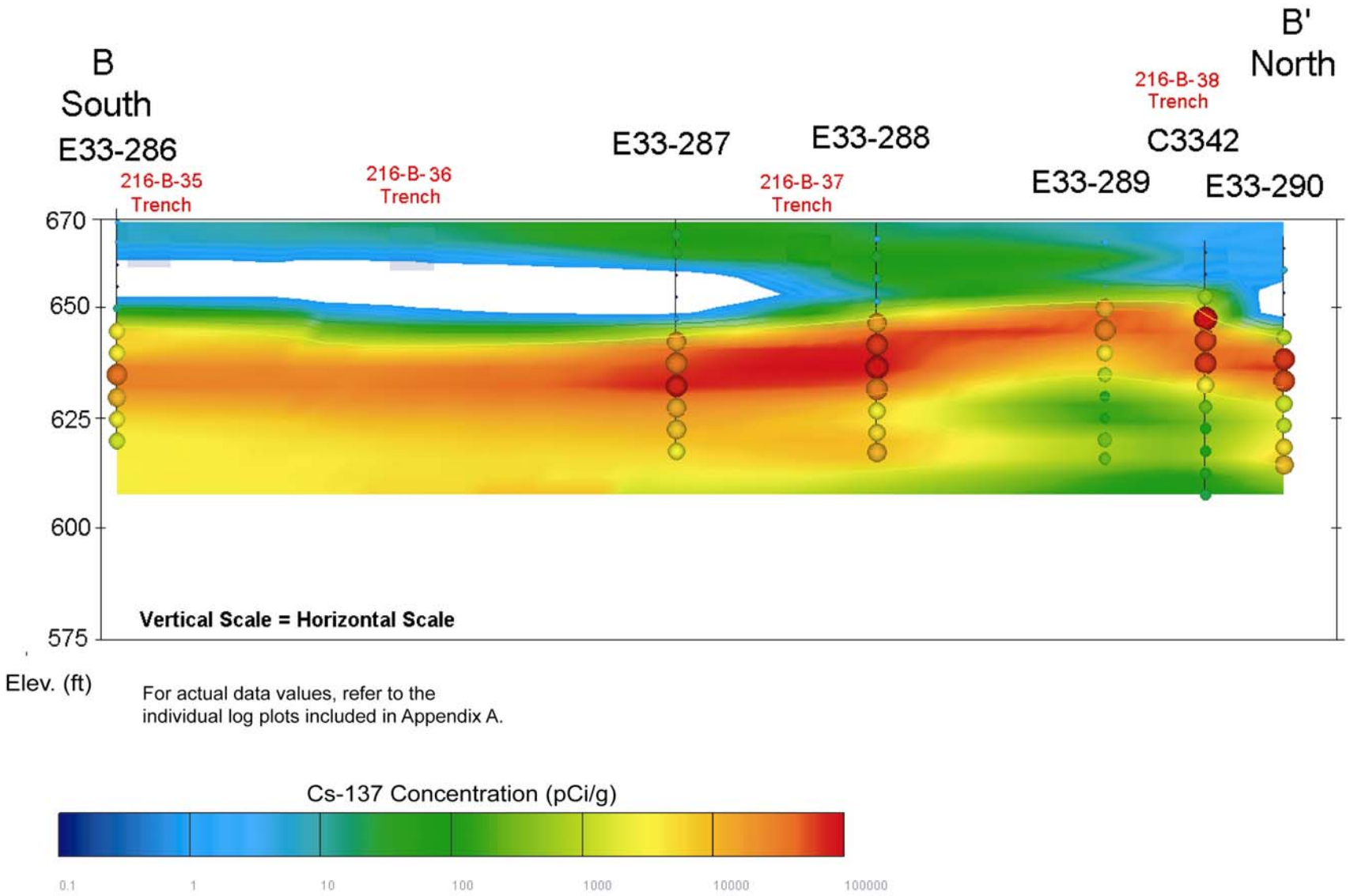


*Figure 15. Visualization of Cross-Section B-B' Showing the Cs-137 Contamination Perpendicular to the 216-B-35 to -38 Trenches*

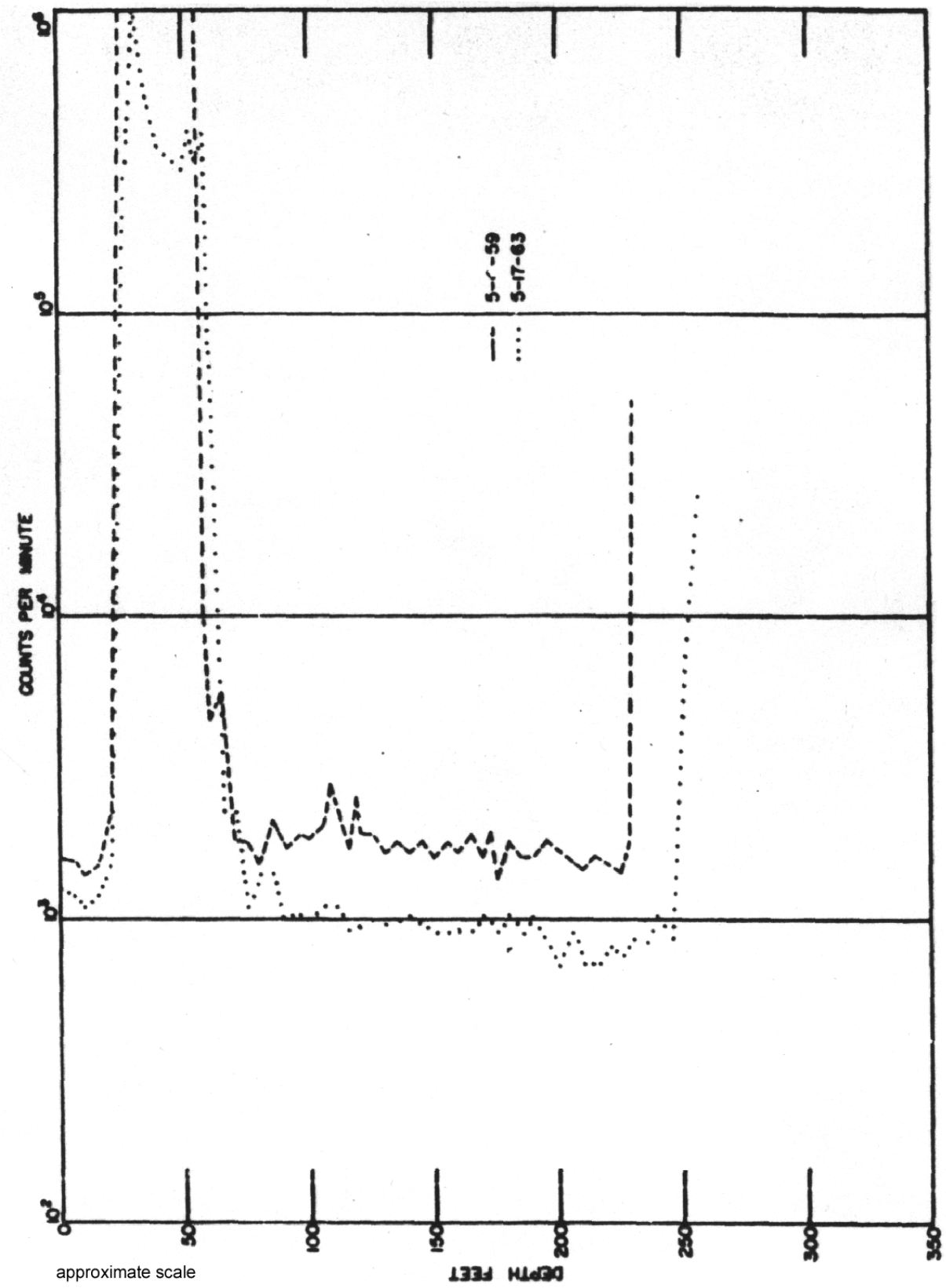


*Figure 16. Groundwater Well 299-E33-8 Scintillation Log*

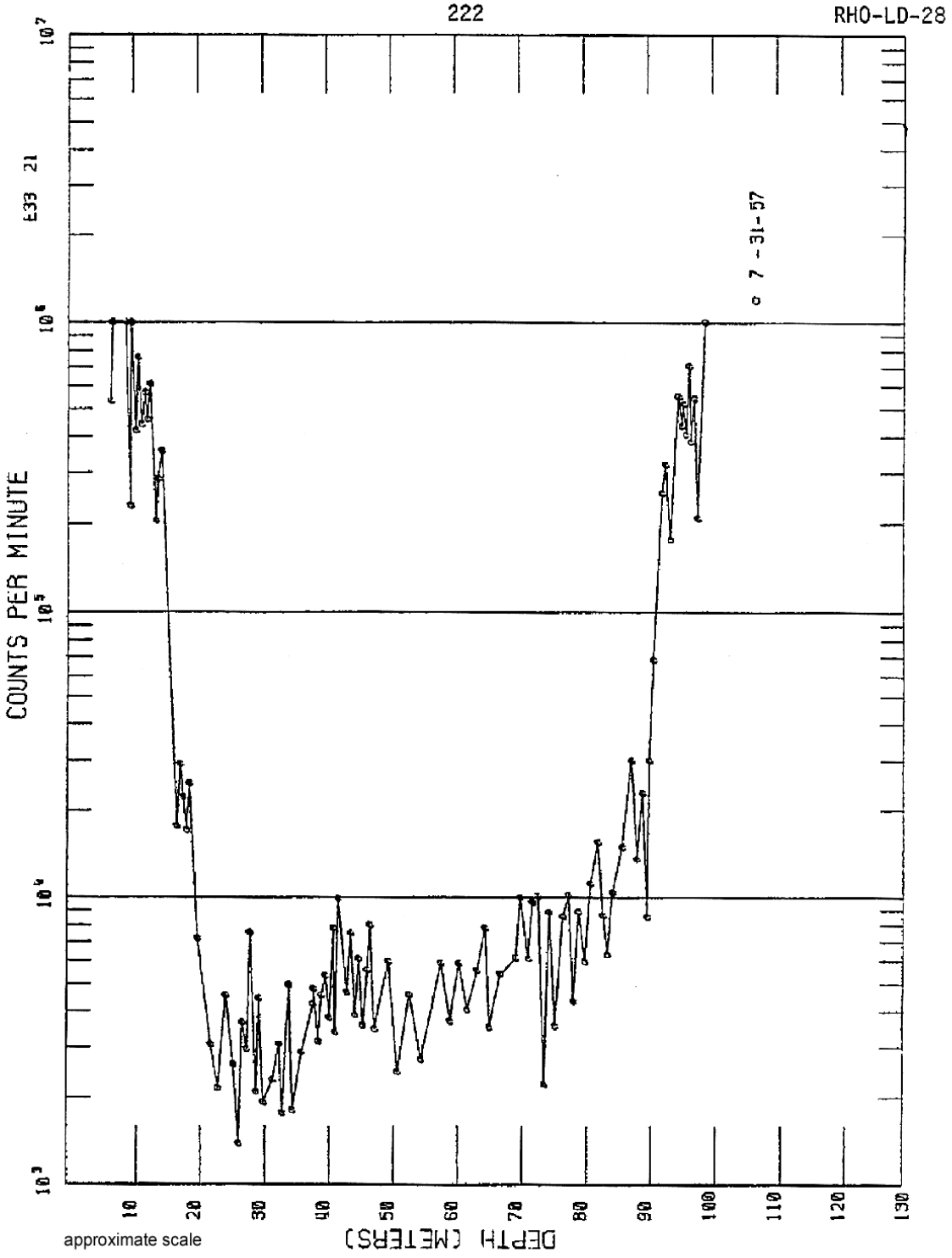


from Additon et al. (1978)

*Figure 17. Groundwater Well 299-E33-21 Scintillation Log*

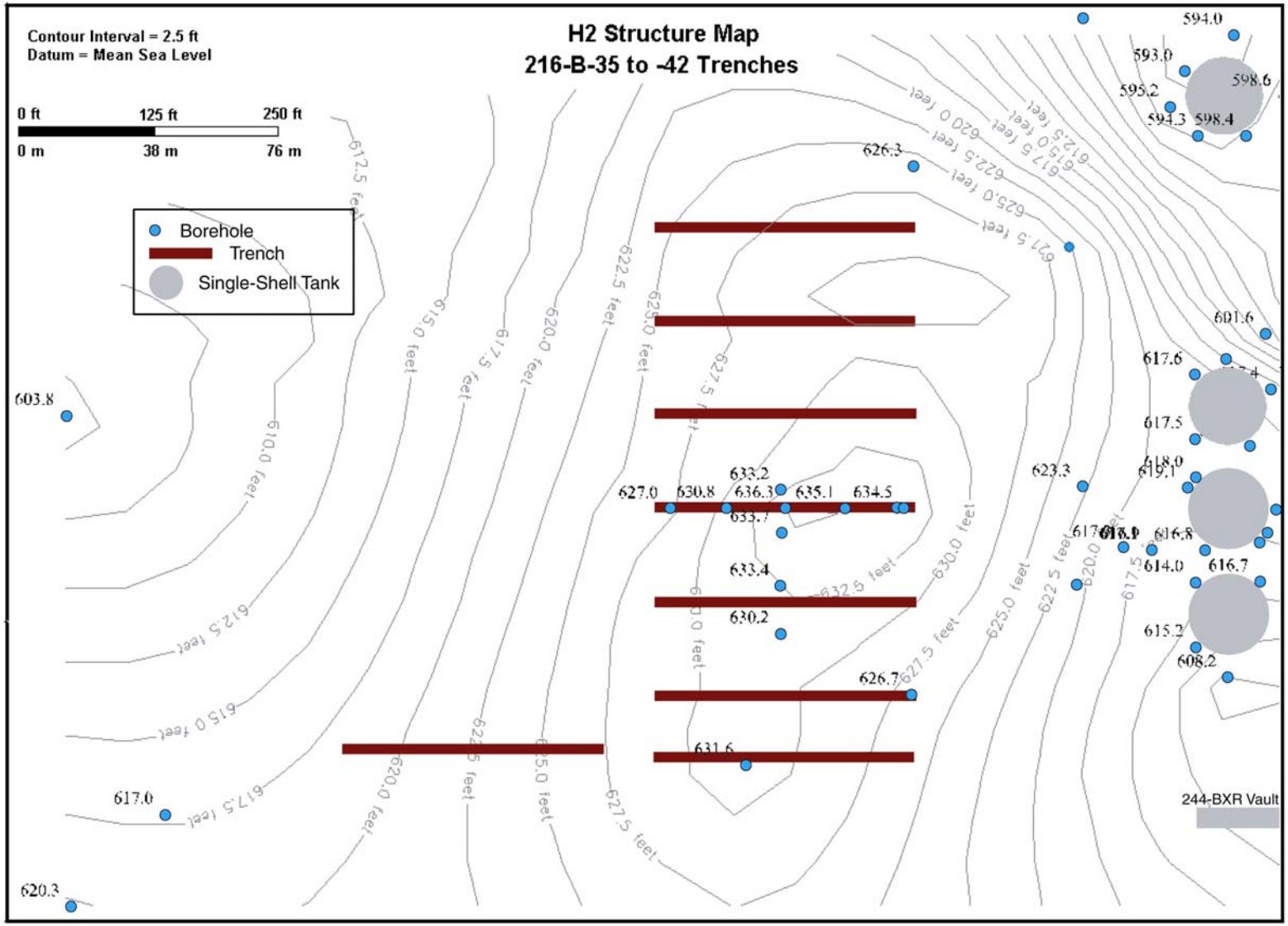


Do not scale this figure

*Figure 18. Top of Hanford H2 Structure Map, 216-B-35 to -42 Trenches*

# References


Additon, M.K., K.R. Fecht, T.L. Jones, and G.V. Last, 1978. *Scintillation Probe Profiles from 200 East Area Crib Monitoring Wells*, RHO-LD-28, Rockwell International, Richland, Washington.

Baker, U.R., B.N. Bjornstad, A.J. Busacca, K.R. Fecht, E.P. Kiver, U.L. Moody, J.G. Rigby, O.F. Stradling, and A.M. Tallman, 1991. "Quaternary Geology of the Columbia Plateau" in Morrison, R.B. (ed.), *Quaternary Non-Glacial Geology: Conterminous U.S.,* Boulder, Colorado, GSA, the Geology of North America, Vol. K-2.

Bergeron, M.P., E.J. Freeman, and S.K. Wurstner. 2001. *Addendum to Composite Analysis for Low-Level Waste Disposal in the 200 Area Plateau of the Hanford Site*, PNNL-11800 Addendum 1, Pacific Northwest National Laboratory, Richland, Washington.

Bjornstad, B.N., K.R. Fecht, and A.M. Tallman, 1987. *Quaternary Stratigraphy of the Pasco Basin, South Central Washington*, RHO-BW-SA-563A, Rockwell Hanford Operations, Richland, Washington.

Bjornstad, B.N., G.V. Last, G.A. Smith, K.A. Lindsey, K.R. Fecht, S.P. Reidel, D.G. Horton, and B.A. Williams, 2002. *Proposed Standardized Stratigraphic Nomenclature for Post-Ringold Sediments Within the Central Pasco Basin*, 2nd draft, Pacific Northwest National Laboratory, Richland, Washington.

Brodeur, J.R., R.K. Price, R.D. Wilson, and C.J. Koizumi, 1993. *Results for Spectral Gamma-Ray Logging of Selected Boreholes for the 200 Aggregate Area Management Study*, WHC-SD-EN-TI-021, Westinghouse Hanford Company, Richland, Washington.

Brown, R.E. and H.G. Rupert, 1948. *Underground Waste Disposal at Hanford Works*, HW-9671, General Electric Hanford Company, Richland, Washington.

Caggiano, J.A., 1996. *Assessment Groundwater Monitoring Plan for Single Shell Tank Waste Management Area B-BX-BY*, WHC-SD-ENV-AP-002, prepared by Westinghouse Hanford Company for the U.S. Department of Energy, Richland, Washington.

Connelly, M.P., J.V. Borghese, C.D. Delaney, B.H. Ford, J.W. Linberg, and S.J. Trent, 1992. *Hydrogeologic Model for the 200 East Groundwater Aggregate Area*, WHC-SD-EN-TI-019, Westinghouse Hanford Company, Richland, Washington.

Delaney, C.D., K.A. Lindsey, and S.P. Reidel, 1991. *Geology and Hydrology of the Hanford Site: A Standardized Text for Use in Westinghouse Hanford Company Documents and Reports*, WHC-SD-ER-TI-0003, Westinghouse Hanford Company, Richland, Washington.

Fecht, K.R., G.V. Last, and K.R. Price, 1977. *Evaluation of Scintillation Probe Profiles from 200 Area Crib Monitoring Wells*, ARH-ST-156, Atlantic Richfield Hanford Company, Richland, Washington.

Fecht, K.R., K.A. Lindsey, B.N. Bjornstad, D.G Horton, G.V. Last, and S.P. Reidel, 1999. *Clastic Injection Dikes of the Pasco Basin and Vicinity, Geologic Atlas Series*, prepared for the U.S. Department of Energy Office of Environmental Restoration, BHI-01103, Rev. 0, Richland, Washington, July.

Glover, D.W., 1985. *Crustal Structure of the Columbia Basin, Washington, From Borehole and Refraction Data*, M.S. thesis, University of Washington (Seattle).

Hartman, M.J. (ed.), 1999. *Hanford Site Groundwater Monitoring for Fiscal Year 1998*, PNNL-12086, Pacific Northwest National Laboratory, Richland, Washington, February.

Hooper, P.R., and V.E. Camp, 1981. "Deformation of the Southeast Part of the Columbia Plateau" in *Geology*, v. 9, p. 323-328.

Hooper, P.R., and R.M. Conrey, 1989. "A Model for the Tectonic Setting of the Columbia River Basalt Eruptions," in Reidel, S.P, and P.R. Hooper (ed.), *Volcanism and Tectonism in the Columbia River Flood-Basalt Province,* Boulder, Colorado, Geological Society of America Special Paper 239, pp. 293-306.

Horton, D.G., and R.R. Randall, 2000. *Results of 1999 Spectral Gamma-Ray and Neutron Moisture Monitoring of Boreholes at Specific Retention Facilities in the 200 East Area, Hanford Site*, PNNL-13077, Pacific Northwest National Laboratory, Richland, Washington.

Koizumi, C.J., 2002. *Hanford Geophysical Logging Project, 2001 Recalibration of Logging Systems for Characterization of Subsurface Contamination at the Hanford Site,* GJO-2002-328-TAR, prepared by MACTEC-ERS, Grand Junction Office, Grand Junction, Colorado.

Ledgerwood, R.K., 1993. *Summaries of Well Construction Data and Field Observations for Existing 200-East Resource Protection*, WHC-SD-ER-TI-007, Revision 0, Westinghouse Hanford Inc., Richland, Washington.

Lindsey, K.A., 1991. *Revised Stratigraphy for the Ringold Formation, Hanford Site, South-Central Washington*, WHC-SD-EN-EE-004, Rev. 0, Westinghouse Hanford Company, Richland, Washington.

Lindsey, K.A., 1996. *The Miocene to Pliocene Ringold Formation and Associated Deposits of the Ancestral Columbia River System, South-Central Washington and North-Central Oregon*, Washington Division of Geology and Earth Resources Open-File Report 96-8.

Lindsey, K.A., and A.G. Law, 1993. Westinghouse Hanford Company Internal Memo, Subject: "Geohydrologic Setting, Flow and Transport Parameters for the Single Shell Tank Farms," 81231-93-060, Westinghouse Hanford Company, Richland, Washington.

Lindsey, K.A., B.N. Bjornstad, J.W. Lindberg, and K.M. Hoffman, 1992. *Geologic Setting of the 200 East Area: An Update*, WHC-SD-EN-TI-012, Rev. 0, Westinghouse Hanford Company, Richland, Washington.

Lindsey, K.A., S.P. Reidel, K.R. Fecht, J.L. Slate, A.G. Law, and A.M. Tallman, 1994. "Geohydrologic Setting of the Hanford Site, South-Central Washington," in *Geologic Field Trips of the Pacific Northwest: 1994 Geological Society of America Annual Meeting*, edited by D.A. Swanson and R.A. Haugerud, Dept. of Geological Sciences, University of Washington, Seattle, Washington, pp. 1C-1 to 1C-16.

Lindsey, K.A., S.E. Kos, and K.D. Reynolds, 2000. *Vadose Zone Geology of Boreholes 299-W22-50 and 299-W23-19 S-SX Waste Management Area, Hanford Site, South-Central, Washington*, RPP-6149, Rev. 0, prepared for CH2M Hill Hanford Group, Richland, Washington, April.

Narbutovskih, S.M., 1998. *Results of Phase I Groundwater Quality Assessment for Single-Shell Tank Waste Management Areas B-BX-BY at the Hanford Site*, PNNL-11826, Pacific Northwest National Laboratory, Richland, Washington.

Pacific Northwest Laboratory (PNL), 1974. *Selected Water Table Contour Maps and Well Hydropraphs for the Hanford Reservation, 1944-1973,* BNWL-B-360, prepared by Pacific Northwest Laboratories for the U.S. Atomic Energy Commission.

Pacific Northwest National Laboratory (PNNL), 1998. *Hanford Site Groundwater Monitoring for Fiscal Year 1997*, PNNL-11793, prepared by Pacific Northwest National Laboratory for the U.S. Department of Energy, Richland, Washington.

Price, W.H., and K.R. Fecht, 1976. *Geology of the 241-BX Tank Farm*, ARH-LD-130, Atlantic Richfield Hanford Company, Richland, Washington.

Raymond, J.R., and V.L. McGhan, 1964. *Scintillation Probe Results 200 Area Waste Disposal Site Monitoring Wells*, HW-84577,General Electric Hanford Atomic Products Operation, Richland, Washington.

Reidel, S.P., 1984. "The Saddle Mountains -- The Evolution of an Anticline in the Yakima Fold Belt," in *American Journal of Science*, v. 284, no. 8, pp. 942-978.

Reidel, S.P., and K.R. Fecht, 1981. "Wanapum and Saddle Mountains Basalt in the Cold Creek Syncline Area" in *Subsurface Geology of the Cold Creek Syncline*, RHO-BWI-ST-14, Rockwell Hanford Operations, Richland, Washington.

Reidel, S.P., K.R. Fecht, M.C. Hagood, and T.L. Tolan, 1989. "The Geologic Evolution of the Central Columbia Plateau," in *Volcanism and Tectonism in the Columbia River Flood-Basalt Province*, Special Paper 239, edited by S.P. Reidel and P.R. Hooper, Geological Society of America, Boulder, Colorado, pp. 247-264.

Reidel, S.P., K.A. Lindsey, and K.R. Fecht, 1992. *Field Trip Guide to the Hanford Site*, WHC-MR-0391, Westinghouse Hanford Company, Richland, Washington.

Reidel, S.P., N.P. Campbell, K.R. Fecht, and K.A. Lindsey, 1994. *Late Cenozoic Structure and Stratigraphy of South-Central Washington*, Washington Division of Geology and Earth Resources Bulletin 80, pp. 159-180.

Rockwell Hanford Operations (Rockwell), 1979. *Geologic Studies of the Columbia Plateau: A Status Report*, RHO-BWI-ST-4, Rockwell Hanford Operations, Richland, Washington.

Rupert, H.G., 1953. *Unconfined Underground Radioactive Waste and Contamination in the 200 Areas*, HW-28471, unknown Hanford Site contractor, Richland, Washington.

Simpson, B.C., R.A. Corbin, and S.F. Agnew, 2001. *Hanford Soil Inventory Model*, BHI-01496, Rev. 0, Bechtel Hanford, Inc., Richland, Washington.

Slate, J.L., 1996. "Buried Carbonate Paleosols Developed in Pliocene-Pleistocene Deposits of the Pasco Basin, South-Central Washington, USA," in *Quaternary International*, Vol. 34-36, pp. 191-196.

U.S. Department of Energy (DOE), 1988. *Consultation Draft Characterization Plan,* DOE/RW-0164, Vol. 1-9, Office of Civilian Radioactive Waste Management, U.S. Department of Energy, Washington, D.C.

_____, 1993a. *B Plant Source Aggregate Area Management Study Report*, DOE/RL-92-05, Rev. 0, U.S. Department of Energy, Richland, Washington.

_____, 1993b. *Phase I Remedial Investigation Report for 200-BP-1 Operable Unit,* Vols. 1 and 2, DOE/RL-92-70, Rev. 0, prepared by Westinghouse Hanford Company for the U.S. Department of Energy, Richland Operations Office, Richland, Washington.

_____, 1998a. *Vadose Zone Characterization Project at the Hanford Tank Farms, BX Tank Farm Report*, GJO-HAN-19, prepared by MACTEC-ERS for the Grand Junction Office, Grand Junction, Colorado.

_____, 1998b. Report to Congress, *Treatment and Immobilization of Hanford Radioactive Tank Waste*, U.S. Department of Energy, July.

_____, 1999. *Hanford Tank Farms Vadose Zone*, *Base Calibration of a High Rate Logging System for Characterization of Intense Radiation Zones in the Hanford Tank Farms*, GJO-HAN-29, prepared by MACTEC-ERS, Grand Junction Projects Office, Grand Junction, Colorado.

_____, 2000. *200-TW-1 Scavenged Waste Group Operable Unit and 200-TW-2 Tank Waste Group Operable Unit RI/FS Work Plan*, DOE/RL-2000-38, Draft A, Richland Operations Office, Richland, Washington.

_____, 2001a. *Hanford Geophysical Logging Project, High Resolution Passive Spectral Gamma-Ray Logging Procedures,* MAC-HGLP 1.6.5, Rev. 0, prepared by MACTEC-ERS, Grand Junction Office, Grand Junction, Colorado.

_____, 2001b. *Hanford Geophysical Logging Project, Project Management Plan,* MAC-HGLP 1.6.2, Rev. 0, prepared by MACTEC-ERS, Grand Junction Office, Grand Junction, Colorado.

U.S. Department of Energy (DOE), 2001c. *Spectral Gamma Vadose Zone Characterization Project, Hanford 200 Areas Vadose Zone Characterization Plan,* MAC-HGLP 1.7.1, Rev. 0, Grand Junction Office, Grand Junction, Colorado.

Waite, J.L., 1991. *Tank Wastes Discharged Directly to the Soil at the Hanford Site,* WHC-MR-0227, Westinghouse Hanford Company, Richland, Washington.

Williams, B.A., B.N. Bjornstad, R. Schalla, W.D. Webber, 2000. *Revised Hydrogeology for the Suprabasalt Aquifer System, 200-East Area and Vicinity, Hanford Site, Washington,* PNNL-12261, Pacific Northwest National Laboratory, Richland, Washington.

Wood, M.I. (Fluor Hanford, Inc.), T.E. Jones (CH2M Hill Hanford Group, Inc.), R. Schalla, B.N. Bjornstad, S.M. Narbutovskih (PNNL), 2000. *Subsurface Conditions Description of the B- BX-BY Waste Management Area*, HNF-5507, CH2M Hill Hanford Group, Inc., Richland, Washington.

# Appendix A
# Spectral Gamma-Ray Logs for Boreholes and Wells in the Vicinity of the 216-B-35 to -42 Trenches

(included on accompanying CD-ROM)